

AD \_\_\_\_\_

Award Number: DAMD17-00-1-0052

TITLE: Permanent Implantation Brachytherapy for Prostate Cancer  
Using a Mixture of Radionuclides with Different Half  
Lives

PRINCIPAL INVESTIGATOR: Ravinder Nath, Ph.D.

CONTRACTING ORGANIZATION: Yale University School of Medicine  
New Haven, Connecticut 06520-8047

REPORT DATE: March 2003

TYPE OF REPORT: Annual

PREPARED FOR: U.S. Army Medical Research and Materiel Command  
Fort Detrick, Maryland 21702-5012

DISTRIBUTION STATEMENT: Approved for Public Release;  
Distribution Unlimited

The views, opinions and/or findings contained in this report are those of the author(s) and should not be construed as an official Department of the Army position, policy or decision unless so designated by other documentation.

20030701 169

# REPORT DOCUMENTATION PAGE

Form Approved  
OMB No. 074-0188

Public reporting burden for this collection of information is estimated to average 1 hour per response, including the time for reviewing instructions, searching existing data sources, gathering and maintaining the data needed, and completing and reviewing this collection of information. Send comments regarding this burden estimate or any other aspect of this collection of information, including suggestions for reducing this burden to Washington Headquarters Services, Directorate for Information Operations and Reports, 1215 Jefferson Davis Highway, Suite 1204, Arlington, VA 22202-4302, and to the Office of Management and Budget, Paperwork Reduction Project (0704-0188), Washington, DC 20503

1. AGENCY USE ONLY (Leave blank)		2. REPORT DATE March 2003	3. REPORT TYPE AND DATES COVERED Annual (1 Mar 02 - 28 Feb 03)	
4. TITLE AND SUBTITLE Permanent Implantation Brachytherapy for Prostate Cancer Using a Mixture of Radionuclides with Different Half Lives			5. FUNDING NUMBERS DAMD17-00-1-0052	
6. AUTHOR(S): Ravinder Nath, Ph.D.				
7. PERFORMING ORGANIZATION NAME(S) AND ADDRESS(ES) Yale University School of Medicine New Haven, Connecticut 06520-8047  E-Mail: ravinder.nath@yale.edu			8. PERFORMING ORGANIZATION REPORT NUMBER	
9. SPONSORING / MONITORING AGENCY NAME(S) AND ADDRESS(ES) U.S. Army Medical Research and Materiel Command Fort Detrick, Maryland 21702-5012			10. SPONSORING / MONITORING AGENCY REPORT NUMBER	
11. SUPPLEMENTARY NOTES				
12a. DISTRIBUTION / AVAILABILITY STATEMENT Approved for Public Release; Distribution Unlimited				12b. DISTRIBUTION CODE
13. Abstract (Maximum 200 Words) (abstract should contain no proprietary or confidential information)  The objective of the project is to test whether the therapeutic effectiveness of permanent implant brachytherapy for prostate cancer can be improved by using a combination of short and long half life radionuclides simultaneously. A theoretical model for continuous low dose rate irradiation using a mixture of radionuclides has been developed. Experiments have been performed using BA1112 tumor cells and Chinese Hamster cells growing in vitro and BA1112 cells growing in vivo as solid tumors in WAG/rij rats. Radiobiology parameters for these cells have been determined and used in the theoretical radiobiology model to improve our understanding of the experimental observations. We have designed and fabricated applicators for in vivo irradiations as well as developed the animal care procedures. We have performed in vivo experiments for tumor growth studies using the BA1112 rat model with <sup>125</sup> I, <sup>103</sup> Pd and a 50:50 mixture of the two. Irradiations at 8 cGy/hr did not result in any tumor cures. At 16 cGy/hr tumor cures were observed in <sup>125</sup> I alone, <sup>103</sup> Pd alone and in the 50:50 mixture.				
14. SUBJECT TERMS: cancer therapy, radiation therapy, radiobiology, radiation physics				15. NUMBER OF PAGES 68
				16. PRICE CODE
17. SECURITY CLASSIFICATION OF REPORT Unclassified	18. SECURITY CLASSIFICATION OF THIS PAGE Unclassified	19. SECURITY CLASSIFICATION OF ABSTRACT Unclassified	20. LIMITATION OF ABSTRACT  Unlimited	

NSN 7540-01-280-5500

Standard Form 298 (Rev. 2-89)  
Prescribed by ANSI Std. Z39-18  
298-102

## Table of Contents

Cover.....	1
SF 298.....	2
Introduction.....	4
Body.....	4
Key Research Accomplishments.....	13
Reportable Outcomes.....	14
Conclusions.....	14
References.....	14
Appendices.....	Six Documents

## INTRODUCTION

The objective of the project is to test whether the therapeutic effectiveness of permanent implant brachytherapy for prostate cancer can be improved by using a combination of short and long half life radionuclides simultaneously. Specific aims of the proposed project are:

1. To test theoretically the potential of a mixture of radionuclides in permanent implants, using the linear quadratic model, as a function of  $T_{pot}$ , potential tumor doubling time.
2. To test experimentally the validity of this concept by in vitro irradiation of BA1112 sarcoma cells at a continuous low dose rate (CLDR) with  $^{125}\text{I}$  (60 d half life),  $^{103}\text{Pd}$  (17 d half life) and a 50:50 mixture of  $^{125}\text{I}$  and  $^{103}\text{Pd}$  under aerobic conditions leading to exponential growth at different rates (from near quiescence to full exponential growth at a maximal rate, with a doubling time of approximately 14 hours).
3. To measure the radiobiology parameters such as alpha, beta, half life of repair for the BA1112 sarcoma cells under different growth conditions and develop a theoretical model to predict expected levels of cell killing using  $^{125}\text{I}$ ,  $^{103}\text{Pd}$  or a mixture of these isotopes.
4. To use immunohistochemical techniques to measure, in solid BA1112 tumors in vivo, the proportion of cells in S phase, the proportion proliferating and non-proliferating cells and the tumor doubling time.
5. To test the therapeutic effectiveness of  $^{103}\text{Pd}$ ,  $^{125}\text{I}$  and a Pd/I mixture in the BA1112 in vivo tumor system;
6. To test the therapeutic effectiveness of  $^{103}\text{Pd}$ ,  $^{125}\text{I}$  and a Pd/I mixture in human prostate carcinoma xenografts in nude mice, using a slow growing and a fast growing carcinoma.
7. To evaluate the clinical potential and feasibility of this approach in the treatment of human prostate cancer.

## BODY OF THE REPORT

We have developed a theoretical radiobiology model for cell killing by continuous low dose rate irradiation (CLDRI) using a mixture of radionuclides. Theoretical studies were performed to investigate the hypothesis and to plan in vitro and animal studies. Experiments have been performed using BA1112 tumor cells and Chinese Hamster cells growing in vitro and BA1112 cells growing in vivo as solid tumors in WAG/rij rats. Radiobiology parameters for these cells have been determined and used in the theoretical radiobiology model to improve our understanding of the experimental observations.



## The linear-quadratic model of cell-killing by CLDRI Using a Mixture of Radionuclides

We have developed a theoretical model for CLDRI using a mixture of radionuclides with different half lives. This model is described in the attached manuscript entitled "Biologically effective dose (BED) for interstitial seed implants containing a mixture of radio-nuclides with different half lives" by Zhe Chen and Ravinder Nath. Briefly, the purpose of this project was to develop a tool for evaluating interstitial seed implants that contain a mixture of radionuclides with different half-lives and to examine the clinical implications of prescribing to an isodose surface for such an implant. Using a generalized equation for the biological effective dose (BED)<sup>1-4</sup>, the effects of cell proliferation and sub-lethal damage repair were examined systematically for implants

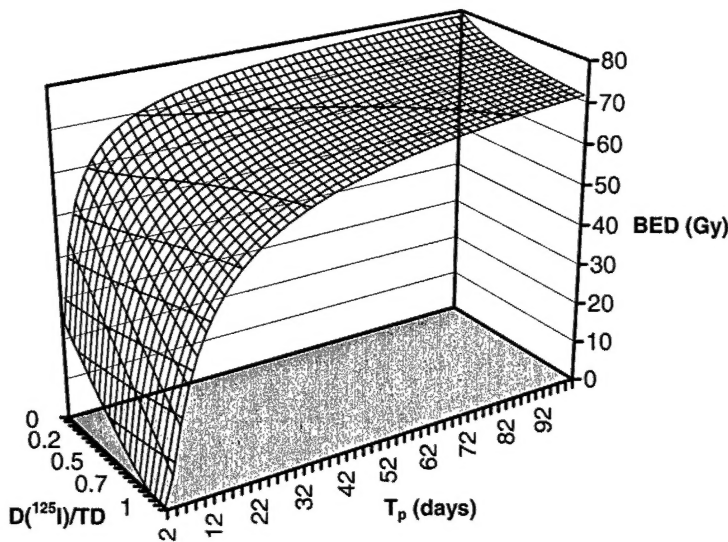


Figure 1

containing a mixture of radionuclides (Figure 1). The results were contrasted with those for implants using a single type of radionuclide. A clinical permanent seed implant that contained a mixture of <sup>125</sup>I and <sup>103</sup>Pd seeds was used to examine the clinical implications of the isodose prescription for such implants. An equation of BED for implants containing any number of radionuclide types

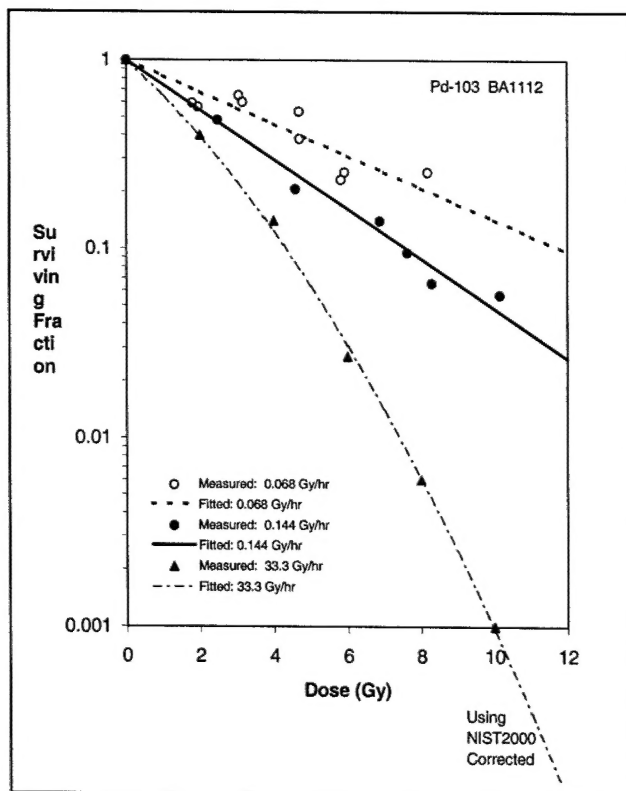
was obtained. For implants containing a mixture of radionuclides with different half-lives such as <sup>125</sup>I and <sup>103</sup>Pd, the dose as well as its temporal delivery pattern to a point is dependent on the relative dose contributions from different types of radionuclide. It can vary from point to point throughout the implant volume. Therefore the quantitative effects of cell proliferation and sub-lethal damage repair are spatially dependent in such an implant. For implants containing a mixture of <sup>125</sup>I and <sup>103</sup>Pd seeds, the prescription to an isodose surface becomes non-unique. If the prescription dose was based on existing clinical experience of using <sup>125</sup>I seeds alone, mixing <sup>103</sup>Pd seeds with <sup>125</sup>I seeds would decrease the cell survival in such implant. On the other hand, if the prescription dose was based on existing clinical experience of using <sup>103</sup>Pd seeds alone, mixing <sup>125</sup>I seeds with <sup>103</sup>Pd seeds in a same implant would create radiobiologically "cold" spots (i.e. an increase in cell survival from the clinical expectation) at locations where a major portion of prescription dose is contributed by the <sup>125</sup>I seeds. For fast-growing tumors, these "cold" spots can become significant. From this theoretical investigation, we conclude that when

cell proliferation and sub-lethal damage repair are present during dose delivery, total dose alone is no longer sufficient for a complete characterization of an interstitial seed implant. In order to avoid radiobiological "cold" spots when radionuclides of different half-lives are mixed in a permanent implant, the dose prescription should be based on the clinical experience of using the longer half-life radionuclide. Biologically effective dose provides a tool to start examining the radiobiological effects of mixing different type of radionuclides in the same implant.

A manuscript has been submitted for publication in the International Journal of Radiation Oncology.

### In vitro CLDRI studies

BA1112 tumors were grown between the ears of the a 14 week old male WAG/rij rats by interdermal inoculation from a single cell suspension of BA1112 cells obtained from a 21 day BA1112 tumor growing on the head of a previously inoculated rat. A tumor cell suspension was made from the BA1112 tumor and between  $1.5 \times 10^5$  and  $5.0 \times 10^5$  cells were plated into petri dishes. These cells were allowed to settle and reach logarithmic growth, (48-72 hrs), before they were used in a continuous low dose rate experiment.



Monolayers of rat rhabdomyosarcoma cells (BA1112) were irradiated in vitro by  $^{103}\text{Pd}$  sources in a polystyrene phantom. Colony formation ability of irradiated cells under aerobic conditions was measured for graded doses, at a dose rate of 6 cGy/hr. Dose to the cell monolayers was determined using  $\text{FeSO}_4$  Fricke dosimetry, with a calculated correction for interface effects due to photoelectric effect in the tissue culture dishes. The sources (up to 60 in one experiment) were arranged in concentric circles in such a way as to provide a dose uniformity of better than  $\pm 5\%$  across the dishes. Some of the results are shown in Figure 2. Comparison of the surviving fraction as a function of dose calculated for the BA1112 cells to

that measured by using CLDRI  $^{103}\text{Pd}$  irradiation is also shown in Figure 2. The lines through the data points represent the calculated survival curves the symbols represent the

measured data. The parameters of  $\alpha$ ,  $\beta$ , repair half-time, and tumor doubling time were determined directly from the measurements performed on the BA1112 cells, as described later in the report.

A manuscript entitled "Dose rate dependence of the relative biological effectiveness of  $^{103}\text{Pd}$  for Continuous Low Dose Rate Irradiation of BA1112 Rhabdomyosarcoma Cells in vitro relative to Acute Exposures" has been prepared for submission to Int. J. Radiat. Oncology. (Appendix II).

### **In vitro studies at an acute dose rate using simulated x-ray beams**

To study the radiobiological characteristics of the cells under acute exposure condition, simulated x-ray beams with average energies equivalent to that emitted by  $^{125}\text{I}$  (27.2 – 35.49 keV with an average of 27.4) and  $^{103}\text{Pd}$  (20 – 22.7 keV with an average of 20.5 keV) were established on a new orthovoltage unit. The simulated beams not only have the average energies similar to that given by the radioactive isotopes but also have a narrow photon energy spectrum. The narrow photon energy spectrum was achieved by optimizing the tube voltage (which determines the upper limit of the produced photon energy) and the added filtration (which filters out the low-energy Bremsstrahlung photons), following the work of Muench et al<sup>5</sup>.

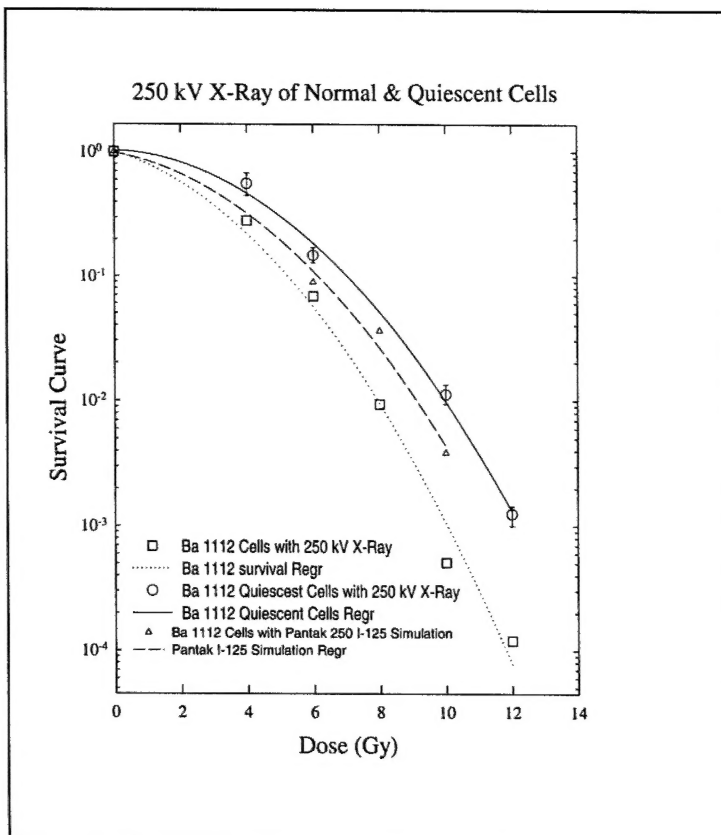
Aluminum filters from Pantak was used to construct a customized filter for the DXT 300 unit that has a desired filtration thickness. A set of aluminum filters (with thickness of 0.1 to 1.0 mm) from Nuclear Associates (AL Filter Set 07-430) were used to determine the half-value-layer (HVL) of a simulated beam using a customized filtration. The thicknesses of the aluminum sheets were measured by using a Mitutoyo micrometer (Serial # 2032360) with accuracy of 0.001 mm). The aluminum HVL for a given beam was determined by in-air ionization chamber measurement under the narrow beam geometry. An air-equivalent Spokas chamber (Exradin, Model No: A1 (0.5 ml, AE plastic)) was used to measure the ionization at a fixed source to chamber distance (SCD) of 50 cm in air. The ionization charge was measured by a Keithley electrometer (model 35614E SN 43075) with –300 V bias potential. Due to the energy dependence of the chamber at the low energies, the measured ionization were converted to corresponding exposure and the HVL is then determined from the relative exposure as a function of aluminum filter thickness. A narrow circular beam, with a diameter of 6 cm at SCD of 50 cm, was generated by using a homemade lead collimator mounted to DXT 300's accessory mount. The aluminum sheets added to the beam for the HVL measurement were taped to the bottom of the lead collimator.

The HVL as a function of mono-energetic photon beam energy for aluminum is taken from Johns and Cunningham<sup>6</sup>. The expected HVL for a simulated  $^{125}\text{I}$  ( $^{103}\text{Pd}$ ) beam with average energy of 27.4 keV (20.5 keV) is 1.84 mm (0.82 mm) aluminum. With the expected HVL in mind, the tube kV, mA and the thickness of the added filtration were optimized for a simulated  $^{125}\text{I}$  and a simulated  $^{103}\text{Pd}$  x-ray beam. The optimum setting determined for the DXT 300 unit is summarized in the following table I.

**Table I. Radiation characteristics of simulated x-ray beams**

Beam	kV	mA	Added Filter (mm AL)	Beam HVL (mm AL)	Energy Homogeneity (%)	Equivalent Energy (keV)	<E> from isotope (keV)
<sup>125</sup> I Equivalent	43	20	3.545	1.851	86.9	27.45	27.4
<sup>103</sup> Pd Equivalent	29	25	1.826	0.82	88.6	20.5	20.5

### In vitro studies for quiescent BA1112 cells



Animals were implanted with transplanted BA1112 rhabdomyosarcomas by inoculation, into a subcutaneous site on the heads. The tumors were allowed to grow for 3 weeks, to an experimental volume of approximately 199-200mm<sup>3</sup>. The animals chosen for the quiescent cell experiments were euthanized by anesthetic overdose and the tumor cells will then be removed using aseptic techniques. A single-cell suspension of tumor cells was suspended, counted, and assayed for viability using the same colony formation assay used for cells in cultures. 1.5 x10<sup>5</sup> cells were plated into a flask with 13 ml of DMEM for cell growth. These cells will

then be passed twice a week for approximately 4-8 passages. The cells are transplanted for 2-4 weeks to assure a homogeneity population of BA1112 cells.

When the first line has reached passage 5 the cells were counted and 1.0x10<sup>7</sup> plated into 5 petri dishes for a cell survival experiments with either normal or quiescent cells. We know from our previous quiescent cell induction experiments that between Days 5-7 were optimal to assure cells in a healthy quiescent state. If we waited past Day 7 we will be in past are optimal window and exhibiting the cell death phase.

The quiescent cells are irradiated on Day 6 or 7, and the response of tumors to irradiation will be assessed by the ability of the BA 1112 tumor cells to form colonies in cell culture after in vitro irradiations. A single-cell suspension of the tumor cells will be counted, and assayed for viability and appropriate cell numbers plated in each petri dish as determined by the specific dose given to the BA1112 cells in the petri dish. Therefore multiple platings from a single cell suspension are mandatory to ensure an adequate countable number of colonies. After these dishes are allowed to grow for 14 days in a controlled environment, 37°C incubator with 95% air/5% CO<sub>2</sub>, they are stained with crystal violet. Analysis of cell yield is performed.

### **Radiological Parameters for CCL-16 and BA1112 cells**

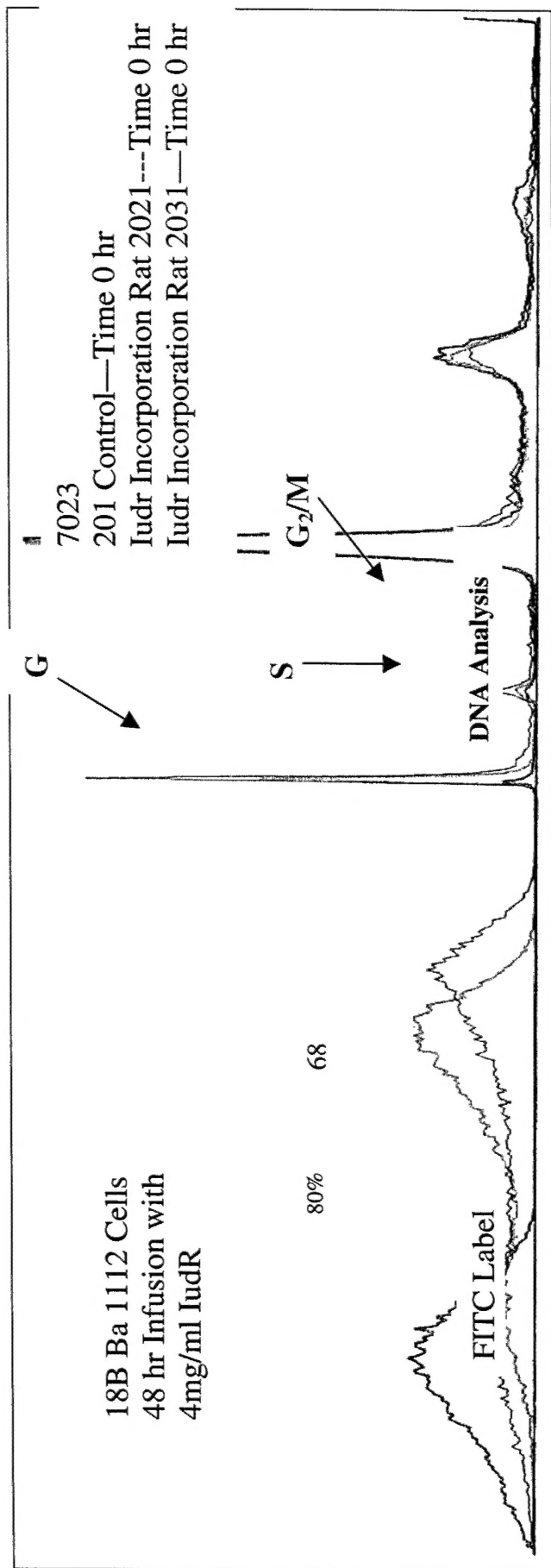
In order to measure the radiological parameters of the cells used in these studies, the acute exposure survival curves were measured using 250 kV x-rays. Split dose experiments were conducted to measure the half time of sublethal damage repair. Results are described in Appendix III and IV. For BA1112 cells the results are summarized in the table below.

#### **Radiobiological Parameters Determined from Acute Exposure Experiments**

Beam	Parameters for Ba-1112				
	$\alpha$ (Gy <sup>-1</sup> )	$\beta$ (Gy <sup>-2</sup> )	$\alpha/\beta$ (Gy)	Tumor Doubling Time (day)	Sub-lethal Damage Repair Half-time (hr)
250 kV old	0.25	0.041	6.1	3.0	0.33
<sup>125</sup> I equivalent	0.26	0.043	6.1	3.0	0.33
<sup>103</sup> Pd equivalent	0.29	0.048	6.1	3.0	0.33
250 kV old	0.23	0.044	5.1	3.0	0.33
<sup>125</sup> I New	0.25	0.044	5.6	3.0	0.33
<sup>103</sup> Pd New	0.32	0.044	7.3	3.0	0.33

### **IUdR and BrdU Labeling For Flow Cytometric Analysis**

We have developed protocols for in vitro IudR labeling and in vivo BrdU labeling for flowcytometric analysis of CCL-116 and BA1112 cells based upon a protocol from Dr. Hong Sun at Yale (Appendix V). Several studies on CCL-116 and BA1112 cells have been performed and results are being analyzed. An example is shown below.

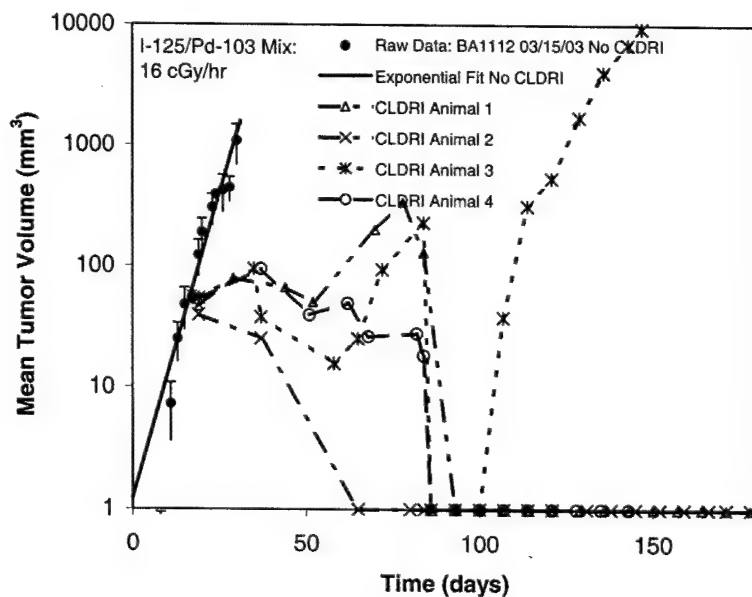


Infused Sample: Iudr Incorporation:	Rat 2021: Time 0 hr:	G <sub>1</sub> = 80%	S = 82%	G <sub>2</sub> M = 78%
	Rat 2031: Time 0 hr:	G <sub>1</sub> = 70%	S = 72%	G <sub>2</sub> M = 68%
Control Sample: Iudr Incorporation:	Rat 201 Time 0 hr:	G <sub>1</sub> = 0.2%	S = 0.3%	G <sub>2</sub> M = 0.3%

### In vivo tumor growth studies

In order to produce a consistent dose distribution to irradiate the tumors transplanted to different animals and to minimize radiation exposure to personnel handling the radioactive seeds, an afterloading seed applicator was designed and fabricated. The applicator was made of polystyrene with loading ports for nine seeds. The central portion of the applicator was open and has a dimension large enough for tumor to grow. Equal source strength was assigned to all nine seeds in order to minimize the possible confusion of handling variable source strengths. The seeding configuration was optimized to produce an, as uniform as possible, dose distribution to the central portion of the applicator and to be usable for both  $^{125}\text{I}$  and  $^{103}\text{Pd}$  seeds. Details are described in Appendix VI.

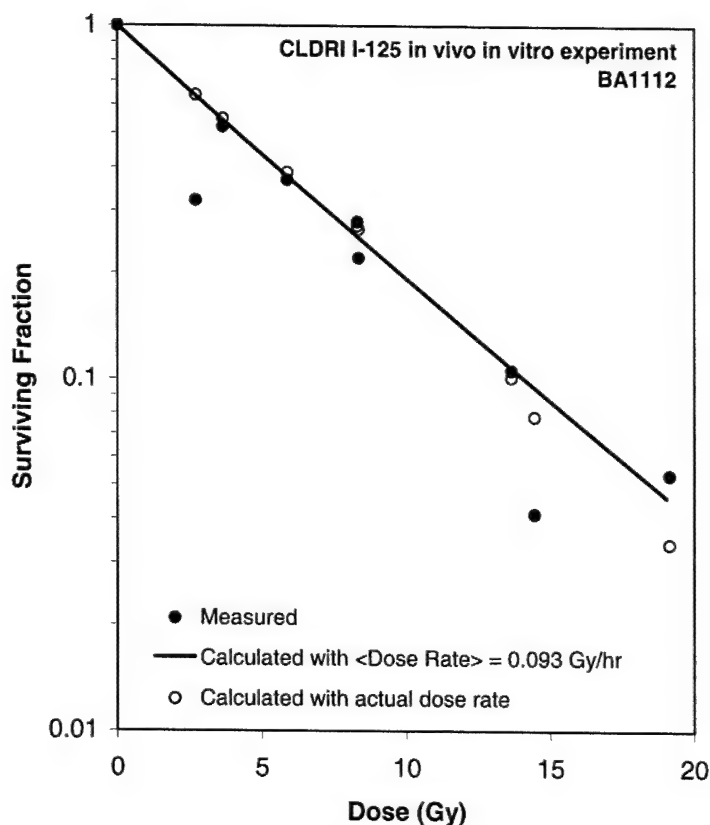
Experiments were conducted using  $^{125}\text{I}$  seeds with an initial dose rate of 8 cGy/hr. Later experiments were conducted at 16 cGy/hr using I-125 alone,  $^{103}\text{Pd}$  alone and a mixture of  $^{125}\text{I}$  and  $^{103}\text{Pd}$  seeds. Typical results are shown in Figures below. Details are described in a manuscript entitled "Development of a Rat Solid Tumor Model for Continuous Low Dose Rate Irradiation Studies using  $^{125}\text{I}$  and  $^{103}\text{Pd}$  Sources" which has been prepared for submission to Int J of Brachytherapy Appendix VI).



### In vivo studies using an in vitro assay



In this experiment, BA1112 tumor cells were irradiated in vivo to graded doses from 2 to 20 Gy. Following irradiation at low dose rate, the tumours were removed and their colony formation ability was measured using our in vitro assay techniques. Figure 11 shows a comparison of the surviving fraction as a function of dose calculated for the BA1112 cells to that measured in an in vivo/in vitro experiment using CLDRI  $^{125}\text{I}$  irradiation. The solid line represent the calculated survival curve using the average initial dose rates used in the experiments. The open circle represent calculation using the actual initial dose rate for each experiment. The parameters of  $\alpha$ ,  $\beta$ , repair half-time, and tumor doubling time were determined directly from the measurements performed on the BA1112 cells (details are provided separately).



### Nude Mice Studies

One of the specific aims in the proposal was to test the therapeutic effectiveness of  $^{103}\text{Pd}$ ,  $^{125}\text{I}$  and a Pd/I mixture in human prostate carcinoma xenografts in nude mice, using a slow growing and a fast growing carcinoma. This was to be followed depending upon the successful completion of the BA112 in rats studies and to be initiated near the end of the project. Some experimental design studies were performed to investigate the feasibility of using the applicator. Several different designs were considered from a



dosimetric point of view. Because of the smaller size of mice and the limitations in reducing the applicator size and weight, we were unable to reach a practical solution. From these initial studies, we have concluded that xenografts studies on nude mice would not be feasible at this stage. A different animal model and brachytherapy applicator would be needed to investigate this issue further.

## KEY RESEARCH ACCOMPLISHMENTS

- A theoretical model based on incomplete repair during CLDRI has been developed for addressing the questions raised in the project. The BED for implants with a mixture of two radionuclides has been derived as an analytical expression. A manuscript describing this work has been published in International Journal of Radiation Oncology (Appendix I).
- Cell survival curves for both  $^{125}\text{I}$  and  $^{103}\text{Pd}$  were measured using monolayers of Chinese hamster cells in a petri dish irradiated at low dose rates using  $^{125}\text{I}$  and  $^{103}\text{Pd}$  sources. The dose sparing effect of 7 cGy/hr relative to 12 cGy/hr can be expressed by dose modifying factors of  $2 \pm 0.6$  and  $1.5 \pm 0.5$  for  $^{103}\text{Pd}$  and  $^{125}\text{I}$ , respectively. The RBEs of  $^{103}\text{Pd}$  relative to  $^{125}\text{I}$  were  $1.2 \pm 0.4$  and  $2.0 \pm 0.5$  for 7 and 12 cGy/hr, respectively. In our system, the RBE of  $^{103}\text{Pd}$  at 19.7 cGy/hr relative to  $^{125}\text{I}$  at 7.72 cGy/hr is estimated to be  $3 \pm 1$ . A manuscript describing this work is in preparation.
- Cell survival curves for  $^{103}\text{Pd}$  were measured using monolayers of BA1112 cells in a petri dish irradiated at low dose rates using  $^{103}\text{Pd}$  sources. An orthovoltage x-ray machine was adapted to produce nearly monoenergetic 21 keV photons, which simulates  $^{103}\text{Pd}$  photon energies. Using this x-ray beam, cell survival curves for the BA1112 cells in a petri dish irradiated at an acute dose rate were also measured. We have successfully tested our theoretical model for predicting the CLDRI survival curves in vitro for  $^{103}\text{Pd}$  sources from the acute dose rate exposure data. A manuscript entitled "Dose rate dependence of the relative biological effectiveness of  $^{103}\text{Pd}$  for Continuous Low Dose Rate Irradiation of BA1112 Rhabdomyosarcoma Cells in vitro relative to Acute Exposures" has been prepared for submission to Int. J. Radiat. Oncology. (Appendix II).
- Cell survival curves for  $^{125}\text{I}$  were measured using of BA1112 cells irradiated in vivo at low dose rate of 8 cGy/hr using the afterloading rat applicator with  $^{125}\text{I}$  sources. An orthovoltage x-ray machine was adapted to produce nearly monoenergetic 28 keV photons, which simulates  $^{125}\text{I}$  photon energies. Using this x-ray beam, cell survival curves for the BA1112 cells in a petri dish irradiated at an acute dose rate were also measured. We are now attempting to test our theoretical model for predicting the CLDRI survival curves in vivo for  $^{125}\text{I}$  sources from the acute dose rate exposure data.
- In order to produce a consistent dose distribution to irradiate the tumors transplanted to different animals and to minimize the radiation exposure to personnel handling the radioactive seeds, an afterloading seed applicator has been designed. Several animals have been treated with CLDRI using these applicators

containing  $^{125}\text{I}$  seeds at 9 cGy/hr. Tumor growth was significantly slowed by CLDRI, from a tumor doubling time of 2.7 days in controls to 13 days in the treated animals. However, no tumor cures were observed at 8 cGy/hr. Further experiments were conducted at 16 cGy/hr for  $^{125}\text{I}$  alone,  $^{103}\text{Pd}$  alone and a 50:50 mixture of  $^{125}\text{I}$  and  $^{103}\text{Pd}$  seeds. Tumor cures were observed at the higher dose rate in all cases. A manuscript entitled "Development of a Rat Solid Tumor Model for Continuous Low Dose Rate Irradiation Studies using  $^{125}\text{I}$  and  $^{103}\text{Pd}$  Sources" has been prepared for submission to Int J of Brachytherapy (Appendix VI).

## REPORTABLE OUTCOMES

A manuscript entitled "Biologically effective dose (BED) for interstitial seed implants containing a mixture of radio-nuclides with different half lives" by Zhe Chen, Ph.D. and Ravinder Nath, Ph.D. has been published in the International Journal of Radiation Oncology. The manuscript is attached as an Appendix I.

A manuscript entitled "Development of a Rat Solid Tumor Model for Continuous Low Dose Rate Irradiation Studies using  $^{125}\text{I}$  and  $^{103}\text{Pd}$  Sources" has been prepared for submission to Int J of Brachytherapy (Appendix VI).

A manuscript entitled "Dose rate dependence of the relative biological effectiveness of  $^{103}\text{Pd}$  for Continuous Low Dose Rate Irradiation of BA1112 Rhabdomyosarcoma Cells in vitro relative to Acute Exposures" has been prepared for submission to Int. J. Radiat. Oncology. (Appendix II).

## CONCLUSIONS

We have made considerable progress towards the specific aims of the project. Theoretical model for continuous low dose rate irradiation using a mixture of radionuclides has been developed. Experiments have been performed using BA1112 tumor cells and Chinese Hamster cells growing in vitro and BA1112 cells growing in vivo as solid tumors in WAG/rij rats. Radiobiology parameters for these cells have been determined and used in the theoretical radiobiology model to improve our understanding of the experimental observations. We have designed and fabricated applicators for in vivo irradiations as well as developed the animal care procedures. We have performed in vivo experiments for tumor growth studies using the BA1112 rat model with  $^{125}\text{I}$ ,  $^{103}\text{Pd}$  and a 50:50 mixture of the two seeds.

## REFERENCES

1. R.G. Dale, Br. J. Radiol. 62, 241-244 (1989).
2. R.G. Dale, Br. J. Radiol. 58, 515-528 (1985).

3. C.C. Ling, Int. J. Radiat. Oncol. Biol. Phys. 23, 81-87 (1992).
4. C.C. Ling, W.X. Li, L.L. Anderson, Int. J. Radiat. Oncol. Biol. Phys. 32, 373-378 (1995).
5. P.J. Muench, A.S. Meigooni, R. Nath, W.L. McLaughlin, Med. Phys. 18, 769-775 (1991)
6. H. Jones and J. R. Cunningham, The Physics of Radiology, 4<sup>th</sup> edition, p. 732, 1983.

## PHYSICS CONTRIBUTION

# BIOLOGICALLY EFFECTIVE DOSE (BED) FOR INTERSTITIAL SEED IMPLANTS CONTAINING A MIXTURE OF RADIONUCLIDES WITH DIFFERENT HALF-LIVES

ZHE CHEN, PH.D., AND RAVINDER NATH, PH.D.

Department of Therapeutic Radiology, Yale University School of Medicine, New Haven, CT

**Purpose:** To develop a tool for evaluating interstitial seed implants that contain a mixture of radionuclides with different half-lives and to demonstrate its utility by examining the clinical implications of prescribing to an isodose surface for such an implant.

**Methods and Materials:** A linear-quadratic model for continuous low dose rate irradiation was developed for permanent implants containing a mixture of radionuclides. Using a generalized equation for the biologically effective dose (BED), the effects of cell proliferation and sublethal damage repair were examined systematically for implants containing a mixture of radionuclides. A head-and-neck permanent seed implant that contained a mixture of  $^{125}\text{I}$  and  $^{103}\text{Pd}$  seeds was used to demonstrate the utility of the generalized BED.

**Results:** An equation of BED for implants containing a mixture of radionuclides with different half-lives was obtained. In such an implant, the effective cell kill was shown to depend strongly on the relative dose contributions from each radionuclide type; dose delivered by radionuclides with shorter half-life always resulted in more cell kill for any given sublethal damage repair and cell proliferation rates. Application of the BED formula to an implant containing a mixture of  $^{125}\text{I}$  and  $^{103}\text{Pd}$  seeds demonstrates that the conventional dose prescription to an isodose surface is not unique for such an implant. When the prescription dose was based on existing clinical experience of using  $^{125}\text{I}$  seeds alone, mixing  $^{103}\text{Pd}$  seeds with  $^{125}\text{I}$  seeds would increase the cell kill. On the other hand, if the prescription dose were based on existing clinical experience of using  $^{103}\text{Pd}$  seeds alone, mixing  $^{125}\text{I}$  seeds with  $^{103}\text{Pd}$  seeds in the same implant would create radiobiologically “cold” spots (i.e., an increase in cell survival) at locations where a major portion of the prescription dose is contributed by the  $^{125}\text{I}$  seeds. For fast-growing tumors, these “cold” spots can become significant.

**Conclusions:** Total dose alone is no longer sufficient for a complete characterization of a permanent seed implant containing a mixture of radionuclides with different half-lives due to the presence of cell proliferation and sublethal damage repair in the protracted dose delivery. BED provides a tool for evaluating the radiobiologic effects of mixing different type of radionuclides in the same implant. When radionuclides of different half-lives are mixed in a permanent implant, using the dose prescription established from existing clinical experience of implants with the longer half-life radionuclide would help to avoid radiobiologic “cold” spots. © 2003 Elsevier Science Inc.

Interstitial implant, Biologically effective dose, Iodine-125, Palladium-103, Brachytherapy, Radiobiology.

## INTRODUCTION

Permanent implantation of encapsulated radioactive seeds in tumors has been used widely as a primary or adjuvant therapy for treating prostate and head-and-neck cancers (1–5). At present, seeds that contain the radionuclide of  $^{125}\text{I}$  or  $^{103}\text{Pd}$  are routinely used in permanent interstitial implants (6).  $^{125}\text{I}$  seed has been introduced since the late 1960s to replace  $^{198}\text{Au}$  seeds due to its long half-life [59.4 days (7)], which is convenient for storage, and its low photon energy, which is easy for radiation protection. It has remained a popular choice for permanent interstitial implant (8).  $^{103}\text{Pd}$  seed, which has an average photon energy close to  $^{125}\text{I}$  and

a shorter decay half-life [16.991 days (7)], was introduced for clinical implant about a decade ago. It is generally considered that  $^{103}\text{Pd}$  seeds, due to their short half-lives, are more effective for fast growing tumors, whereas  $^{125}\text{I}$  seeds are better for slow growing tumors (9). The decision regarding which radionuclide to use for a given implant has been influenced largely by the historical development of radioactive seeds and, recently, by the radiobiologic considerations for each radionuclide (9). Nonetheless, seeds containing different radionuclide types have never been reported in the same clinical implant. For tumors that may contain both fast and slow growing cells, it would seem desirable to use

Reprint requests to: Ravinder Nath, Ph.D., Department of Therapeutic Radiology, Yale University School of Medicine, 333 Cedar Street, New Haven, CT 06510. Tel: (203) 688-2951; Fax: (203) 737-4252; E-mail: Ravinder.Nath@yale.edu

Supported in part by DOD grant DAMD 17-00-1-0052.

**Acknowledgment**—The authors would like to thank Dr. Y. Son for many interesting and helpful discussions on the clinical head-and-neck implant used as an example in this article.

Received Mar 26, 2002, and in revised form Sep 17, 2002. Accepted for publication Oct 14, 2002.

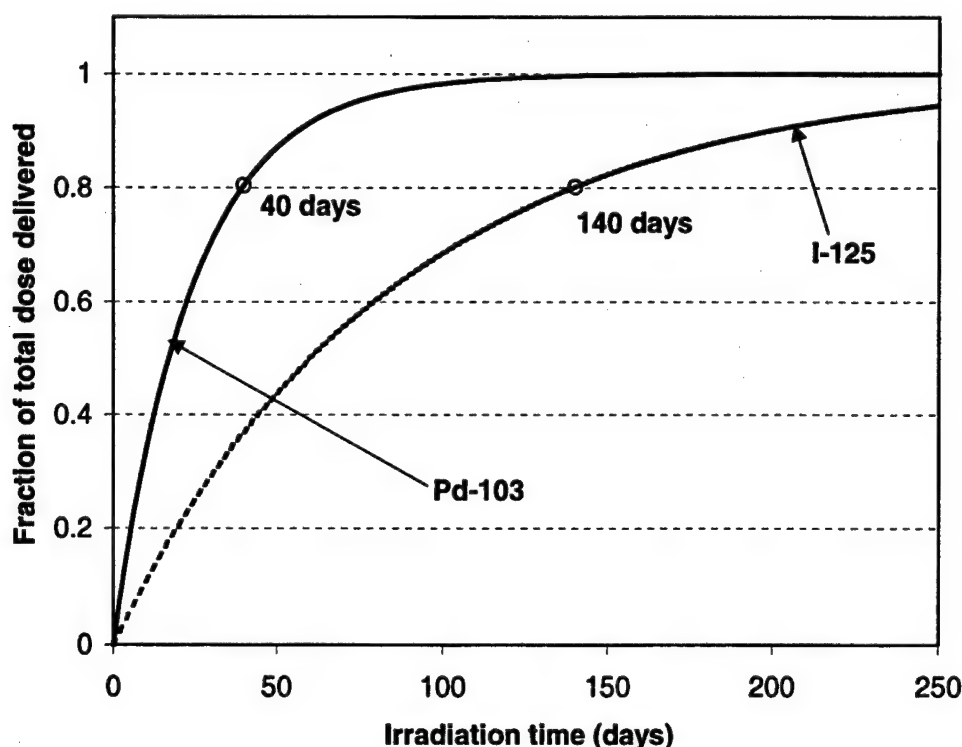


Fig. 1. Accumulative dose delivered as a function of implant time for  $^{125}\text{I}$  and  $^{103}\text{Pd}$  implants. Note that the vertical axis was plotted as the ratio of delivered dose to the dose to full decay.

a mixture of short and long half-life radionuclides (e.g.,  $^{103}\text{Pd}$  and  $^{125}\text{I}$ ) in the same tumor volume. Mixing seeds of different half-lives in the same implant, however, requires new tools to evaluate the clinical impact of the resulting implant. The main goal of this study is to present a tool for evaluating this type of implant and to demonstrate its utility by examining the appropriateness of keeping isodose prescription in such an implant.

The need for a tool, other than the delivered dose, stems from the well-known observation in radiobiology that the cell survival in a permanent interstitial implant depends not only on the total dose but also on the temporal pattern of dose delivery (9–15). For implants containing a single type of radionuclide, the temporal pattern of dose delivery is characterized by a simple exponential reduction of dose rate as a function of time. Figure 1 illustrates the dose delivered as a function of implant time for a  $^{125}\text{I}$  and a  $^{103}\text{Pd}$  implant. The time required to deliver, for example, 80% of dose to full decay differs by a factor of more than 3 (about 140 days for  $^{125}\text{I}$  implants and about 40 days for  $^{103}\text{Pd}$  implants). This difference in the rate of dose delivery (caused by the different decay half-lives) can result in very different clinical responses for a given total dose when the surviving cells in the irradiated volume are continuously proliferating and the sublethally damaged cells can be repaired during the protracted dose delivery (9, 11, 12). Indeed, this consideration has led the prescription dose for  $^{103}\text{Pd}$  seed implants in monotherapy for prostate cancer to 125 Gy, considerably less than the 145 Gy normally prescribed for  $^{125}\text{I}$  implants. When seeds of different half-lives are mixed in the same

implant, the temporal dose delivery pattern to a point within the implant is now defined by the decay characteristics of all radionuclide types that contribute doses to it. The resulting temporal pattern becomes complex (can be nonexponential), and its form varies throughout the implant volume (as a function of seed locations). To properly evaluate such an implant, a tool that can capture the interplay between the complex temporal dose delivery pattern and the underlying tissue radiobiology is needed.

The concept of biologically effective dose (BED) has been used as a surrogate of the biologic responses to ionizing radiation (13–15). For a course of fractionated radiotherapy or brachytherapy, the surviving fraction of the irradiated cell ( $S$ ) is directly linked to BED as

$$S = e^{-\alpha \text{BED}} \quad (1)$$

where  $\alpha$  characterizes the radiosensitivity of cells. The linear-quadratic (LQ) cell survival model has been used by many investigators to calculate the BED for acute, fractionated, and protracted dose delivery (9–15). For protracted irradiation at a constant dose rate, Thames has extended the LQ model for acute irradiation to take into account the kinetics of sublethal damage repair during the dose delivery (13). Later, Dale derived an analytic formula of BED for continuous irradiation with exponentially decreasing dose rate as encountered in brachytherapy with short-lived radionuclides (11, 12). Dale's formulation, fundamentally equivalent to the incomplete

repair model (13), takes into account both the cell proliferation and sublethal damage repair during the dose delivery characterized by a simple exponential function. Ling has used the model to study the relative radiobiologic effectiveness (RBE) of permanent implants using  $^{198}\text{Au}$ ,  $^{125}\text{I}$ , or  $^{103}\text{Pd}$  seeds (9) and to examine the biologic effects of dose heterogeneity inherent in interstitial implants (16). In this article, we generalize Dale's BED formula for implants containing a mixture of radionuclides with different half-lives. The potential of using the generalized BED formula as a tool for evaluating implants containing a mixture of radionuclides is examined. Its usage is demonstrated by examining the clinical implications of isodose prescription for a head-and-neck implant containing a mixture of  $^{125}\text{I}$  and  $^{103}\text{Pd}$  seeds.

## METHODS AND MATERIALS

### Implants containing a mixture of radionuclides

For simplicity, let us consider an implant containing two types of radionuclides (e.g.,  $^{125}\text{I}$  and  $^{103}\text{Pd}$ ). Assume that there are  $N_1$  seeds of radionuclide type 1 and  $N_2$  seeds of radionuclide type 2. In such an implant, the instantaneous dose rate to a point  $\vec{r}$  at time  $t$  after implantation is given by

$$\dot{D}(\vec{r}, t) = \sum_{i=1}^2 \dot{D}_{0i}(\vec{r}) e^{-\lambda_i t} \quad (2a)$$

where  $\dot{D}_{0i}(\vec{r})$  denotes the total initial dose rate produced by the seeds of radionuclide type  $i$ . It depends on the spatial locations of all type  $i$  seeds. It is clear from Eq. 2a that the overall temporal pattern in such an implant depends on the value of  $\dot{D}_{0i}(\vec{r})$ , which can be variable throughout the implant volume. For point-like sources,  $\dot{D}_{0i}(\vec{r})$  is approximately equal to (17)

$$\dot{D}_{0i}(\vec{r}) \approx \sum_{l=1}^{N_i} \frac{S_{il} \Lambda_i r_0^2}{|\vec{r}_{il} - \vec{r}|^2} g_i(|\vec{r}_{il} - \vec{r}|) (\bar{\phi}_{an})_i \quad (2b)$$

In the above equations, the index  $i$  labels the radionuclide type and  $l$  labels the individual seeds.  $S_{il}$  denotes the air-kerma strength for the seed  $l$  of radionuclide type  $i$ .  $\Lambda_i$ ,  $\lambda_i$ ,  $(\bar{\phi}_{an})_i$ , and  $g_i(r)$  denote the dose rate constant, the radioactive decay constant, the anisotropy constant, and the radial dose function, respectively, for the seeds of radionuclide type  $i$ .  $r_0$  denotes the reference distance (usually 1 cm) at which the dose rate constant was determined. In this work, the delivered dose, isodose distribution, and dose-volume histograms used in conventional implant dose evaluation were computed by using Eq. 2 with appropriate parameters for  $^{125}\text{I}$  and  $^{103}\text{Pd}$  seeds (17).

### Linear-quadratic model for CLDRI

Dale's work on BED for implants containing a single type of radionuclide (11, 12) is generalized in this paper for implants containing a mixture of radionuclides of different

half-lives. To model the kinetics of sublethal damage repair, Dale has invoked the assumption that radiation-induced cell inactivation is caused by the damage of two critical targets in a cell to model the kinetics of sublethal damage repair. Under this assumption, when a radiation event damages only one critical target, the cell is considered sublethally damaged, which is repairable. Cell kill occurs only when the other critical target is damaged before the existing damage is fully repaired. By assuming sublethal damage repairs exponentially with time, i.e., if a sublethal damage was inflicted at time  $t_0$ , then the probability for it persisting to time  $t$  is  $e^{-\mu(t-t_0)}$ , the rate of sublethal damage repair can be characterized by a single parameter, repair half-time

$T_{1/2}^{(R)} = \frac{\ln 2}{\mu}$ . Average repair half-times reported for mammalian normal and tumor tissues vary from 0.5 to 3 h with normal tissues usually possessing longer repair half-time (18). For "generic" tumors, a repair half-time of 1.5 h has often been used in model calculation (19). The rate of cell proliferation was also modeled by a single parameter, the tumor potential doubling time  $T_p$ . This model assumes that the cells in a target volume all proliferate at the same rate and cell loss from the tumor volume is negligible. The tumor potential doubling time is tumor-type dependent and may vary from patient to patient even among the same tumor type. For squamous cell head-and-neck cancer, a "typical"  $T_p$  of 5 days has been quoted in literature (19). For prostate carcinoma,  $T_p$  values ranging from 10 to 60 days have been reported in the literature (20). Using these simple models for sublethal damage repair and cell proliferation, Dale derived an analytic expression of BED for interstitial implants containing a single type of radionuclide as follows,

$$\text{BED} = D(T_{\text{eff}}) \text{RE} - \frac{0.693 T_{\text{eff}}}{\alpha T_p} \quad (3)$$

where RE is given by

$$\text{RE} = 1 + 2 \left( \frac{\beta}{\alpha} \right) \frac{\gamma}{D(T_{\text{eff}})} \quad (4a)$$

with

$$\gamma = \frac{\dot{D}_0^2}{\mu - \lambda} \left\{ \frac{1}{2\lambda} (1 - e^{-2\lambda T_{\text{eff}}}) - \frac{1}{\lambda + \mu} (1 - e^{-(\mu + \lambda) T_{\text{eff}}}) \right\} \quad (4b)$$

In the above equations,  $\dot{D}_0$  denotes the initial dose rate,  $\dot{D}(T_{\text{eff}}) = \frac{\dot{D}_0}{\lambda} (1 - e^{-\lambda T_{\text{eff}}})$  is the dose delivered up to  $T_{\text{eff}}$  and  $\alpha$  and  $\beta$  are coefficients of the LQ model. The effect of sublethal damage repair is captured by the factor RE, and the effect of cell proliferation is characterized by the second term on the right-hand side of Eq. 3. This analytic form of



BED has enabled a systematic examination of the interplay between the radioactive half-life and the underlying sublethal damage repair and cell proliferation rates. Many investigators have discussed the use of this BED for implants containing a single type of radionuclide (9, 11, 12, 16, 18, 19, 21). In this paper, a generalized form of Eq. 4 is derived for implants containing a mixture of any number of radionuclides with different half-lives.

## RESULTS

### *BED for implants containing a mixture of radionuclides with different half-lives*

Following Dale's work, a generalized BED for implants containing a mixture of radionuclides with different half-lives was obtained (see Appendix for details of derivation). For an implant mixed with two different half-lives, the  $\gamma$  in Eq. 4 is replaced by

$$\begin{aligned} \gamma = & \frac{\dot{D}_{01}^2}{\mu - \lambda_1} \left\{ \frac{1}{2\lambda_1} (1 - e^{-2\lambda_1 T_{eff}}) - \frac{1}{\lambda_1 + \mu} (1 - e^{-(\mu + \lambda_1) T_{eff}}) \right\} \\ & + \frac{\dot{D}_{02}^2}{\mu - \lambda_2} \left\{ \frac{1}{2\lambda_2} (1 - e^{-2\lambda_2 T_{eff}}) - \frac{1}{\lambda_2 + \mu} (1 - e^{-(\mu + \lambda_2) T_{eff}}) \right\} \\ & + \frac{\dot{D}_{01} \dot{D}_{02}}{\mu - \lambda_1} \left\{ \frac{1}{\lambda_1 + \lambda_2} (1 - e^{-(\lambda_1 + \lambda_2) T_{eff}}) - \frac{1}{\lambda_2 + \mu} (1 - e^{-(\mu + \lambda_2) T_{eff}}) \right\} \\ & + \frac{\dot{D}_{01} \dot{D}_{02}}{\mu - \lambda_2} \left\{ \frac{1}{\lambda_1 + \lambda_2} (1 - e^{-(\lambda_1 + \lambda_2) T_{eff}}) - \frac{1}{\lambda_1 + \mu} (1 - e^{-(\mu + \lambda_1) T_{eff}}) \right\} \end{aligned} \quad (5)$$

where  $\dot{D}_{01}$  and  $\dot{D}_{02}$  denote the initial dose rates, at the point of calculation, produced by seeds containing radionuclide type 1 and 2, respectively; and

$$D(T_{eff}) = \frac{\dot{D}_{01}}{\lambda_1} (1 - e^{-\lambda_1 T_{eff}}) + \frac{\dot{D}_{02}}{\lambda_2} (1 - e^{-\lambda_2 T_{eff}}).$$

Equation 5 is one of the main results of this work. Its general property and application to a clinical implant are discussed in the remainder of this section.

### *BED as a function of sublethal damage repair*

The effects of sublethal damage repair for permanent implants containing seeds of different half-lives can be examined under the condition of  $T_p = \infty$ , i.e., no cell

proliferation. In this case, the  $T_{eff}$  is infinite and Eq. 5 becomes

$$\begin{aligned} RE = 1 + \frac{\beta}{\alpha} \times \\ \frac{\frac{\dot{D}_{01}^2}{\lambda_1(\lambda_1 + \mu)} + \frac{\dot{D}_{02}^2}{\lambda_2(\lambda_2 + \mu)} + 2 \frac{\dot{D}_{01} \dot{D}_{02} (\lambda_1 + \lambda_2 + 2\mu)}{(\lambda_1 + \lambda_2)(\lambda_1 + \mu)(\lambda_2 + \mu)}}{\frac{\dot{D}_{01}}{\lambda_1} + \frac{\dot{D}_{02}}{\lambda_2}} \end{aligned} \quad (6)$$

for an implant containing two different half-lives. BED is simply the product of the total dose and RE. Figure 2 plots the RE as a function of repair half-time for an implant containing a mixture of  $^{125}\text{I}$  and  $^{103}\text{Pd}$  seeds for a fixed total dose. Two general properties are conveyed by this figure: First, at a given repair half-time, the RE, or BED, is a function of relative dose contributions from the two types of seeds. By varying the relative dose contribution from  $^{125}\text{I}$  and  $^{103}\text{Pd}$  seeds, the BED for the mixed-seed implant can be varied continuously from that of using  $^{125}\text{I}$  alone to that of using  $^{103}\text{Pd}$  alone. Therefore, the BED in such an implant will be highly dependent on the locations of the implanted seeds. Second, the BED is larger when the total dose is delivered solely by the radionuclide with shorter half-life ( $^{103}\text{Pd}$  in this case). This point is further illustrated in Fig. 3 in which the RE associated with total dose delivered by either  $^{125}\text{I}$  or  $^{103}\text{Pd}$  alone is plotted from  $T_{1/2}^{(R)} = 0$  to  $T_{1/2}^{(R)} = \infty$ . If sublethal damage can be repaired instantaneously (i.e.,  $T_{1/2}^{(R)} = 0$ ) or is nonrepairable (i.e.,  $T_{1/2}^{(R)} = \infty$ ), no difference in cell kill exists between different radionuclides. In general, implants with radionuclide of shorter half-life exhibit more effective cell kill for the same delivered dose. This advantage of using shorter half-life radionuclide would increase initially as repair half-time increases and would diminish eventually when sublethal damage becomes irreparable.

### *BED as a function of cell proliferation*

The presence of cell proliferation would always reduce the magnitude of BED, because part of the delivered dose has to counter the repopulated cells. The amount of reduction,  $0.693U(\alpha T_p)$ , depends on both the proliferation rate  $[0.693/(\alpha T_p)]$  and the implant duration ( $t$ ). If the proliferation rate remains the same during the dose delivery, there would exist a time at which the cell inactivation rate induced by the decaying dose rate would become less than the proliferation rate. Beyond this time, there would be no net cell kill from the remaining dose delivered. The time at which the cell-kill rate equals the proliferation rate is defined as the effective treatment time  $T_{eff}$  (12). Figure 4 plots the BED calculated at  $T_{eff}$  as a function of the potential tumor doubling time and the relative dose contributions in an implant with mixed  $^{125}\text{I}$  and  $^{103}\text{Pd}$  seeds. A repair half-life of 1.5 h and an  $\alpha/\beta$  of 10 were used in the calculation.

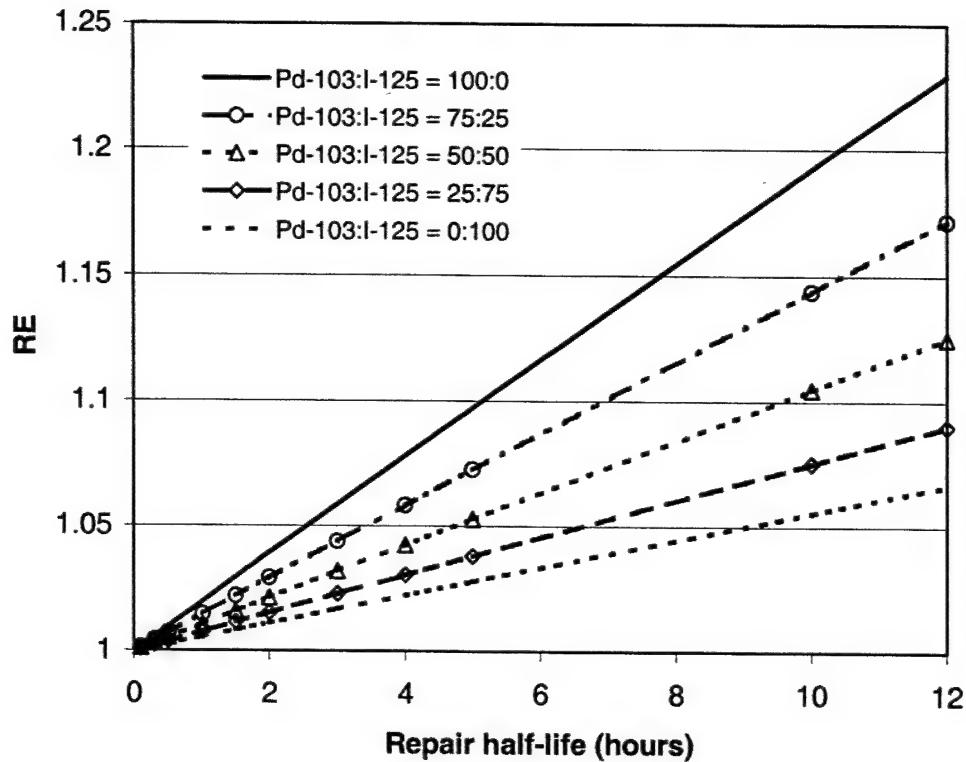


Fig. 2. Relative effectiveness, RE, calculated as a function of repair half-time for implants using a mixture of  $^{125}\text{I}$  and  $^{103}\text{Pd}$  seeds. The BED is the product of RE and the total delivered dose.

Total delivered dose is 80 Gy. When the relative dose contribution by  $^{125}\text{I}$  and  $^{103}\text{Pd}$  seeds is fixed, the BED is shown to increase with  $T_p$ . For a given  $T_p$ , BED is always larger when the same dose is delivered by the radionuclide with shorter half-life ( $^{103}\text{Pd}$  in this case). The difference in BED between dose delivered by  $^{103}\text{Pd}$  and  $^{125}\text{I}$  alone is most significant for fast growing tumors and becomes less significant for slower growing tumors.

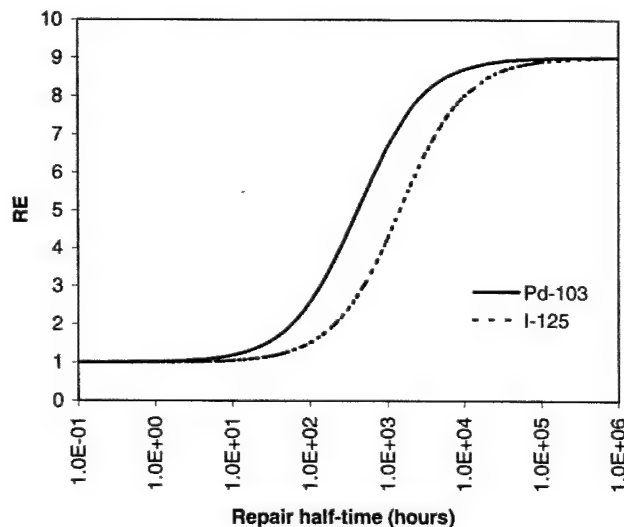


Fig. 3. Relative effectiveness (RE) over the entire range of possible repair half-time for implants using  $^{125}\text{I}$  or  $^{103}\text{Pd}$  alone.

#### *An application of the generalized BED: Inadequacy of isodose prescription in mixed seed implant*

The basic issue regarding the isodose prescription for an implant containing seeds of different half-lives is as follows. For a permanent implant using only a single type of radionuclide, the total dose, TD, at any given point is related to the initial dose rate,  $\dot{D}_0$ ,

$$TD = 1.44T_{1/2}\dot{D}_0 \quad (7)$$

For this type of implant, a prescription to an isodose surface is equivalent to a prescription to an isodose rate surface. In other words, the initial dose rate is fixed once a prescription of total dose is established. The temporal dose delivery pattern in such an implant follows a simple exponential function and is the same throughout the implant volume. For an implant containing a mixture of two radionuclides, however, Eq. 7 becomes

$$TD = 1.44T_{1/2}^{(1)}\dot{D}_0^{(1)} + 1.44T_{1/2}^{(2)}\dot{D}_0^{(2)} \quad (8)$$

The total dose is now dependent on the initial dose rates,  $\dot{D}_0^{(1)}$  and  $\dot{D}_0^{(2)}$ , produced by the two types of radionuclide, respectively. According to Eq. 8, a prescription to an isodose surface can now be fulfilled by many different combinations of  $\dot{D}_0^{(1)}$  and  $\dot{D}_0^{(2)}$ . Therefore the prescription to an isodose surface is not unique with respect to the initial dose rates produced by the two types of radionuclides. Further-



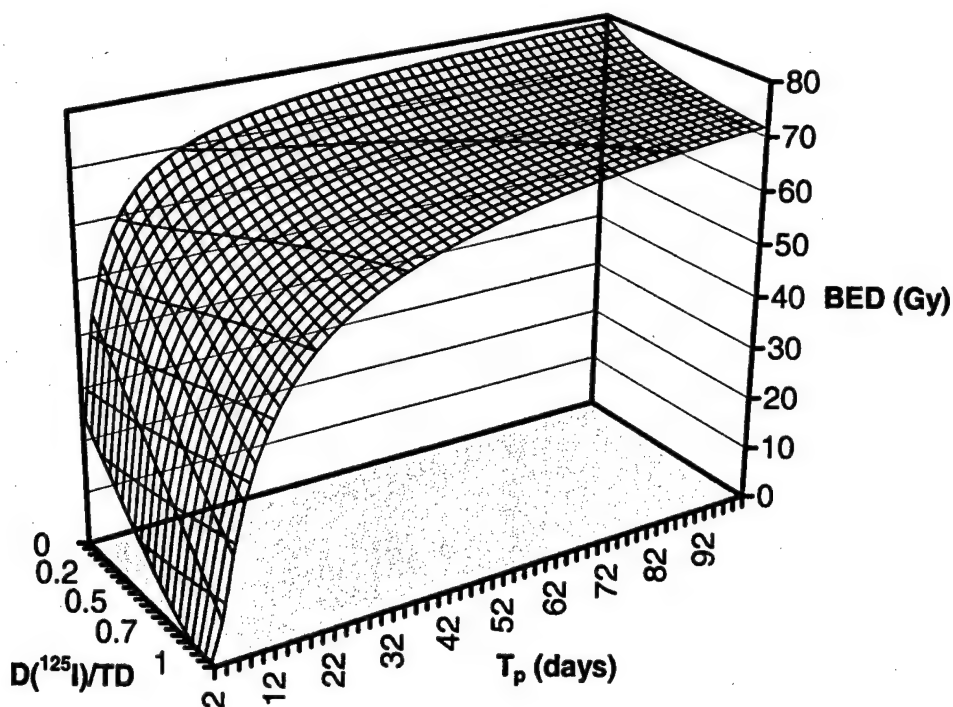


Fig. 4. BED for an 80 Gy implant using a mixture of  $^{125}\text{I}$  and  $^{103}\text{Pd}$  seeds plotted as a function of tumor potential doubling time  $T_p$  and the fraction of total dose delivered from the  $^{125}\text{I}$  seeds. A sublethal damage repair half-life of 1.5 h and a  $\alpha/\beta$  of 10 for tumor were used in the calculation.

more, the overall temporal pattern of dose delivery is now variable throughout the implant volume, determined by the sum of two exponential functions with variable relative weightings.

The clinical implications of prescribing to an isodose surface for such an implant can be examined using the generalized BED formula. Let us take a clinical implant performed on a 45-year-old male patient who presented with cancer of the larynx as an example. The permanent seed implant to the postpharyngeal wall used 10  $^{125}\text{I}$  seeds and 23  $^{103}\text{Pd}$  seeds. Initial source strength was 0.64 U for  $^{125}\text{I}$  seeds and 0.88 U for  $^{103}\text{Pd}$  seeds. Figure 5 shows the isodose lines (to full decay), in the  $x$ - $y$  plane through the center of the implant, contributed by the  $^{125}\text{I}$  seeds alone (top panel), the  $^{103}\text{Pd}$  seeds alone (middle panel), and by both  $^{125}\text{I}$  and  $^{103}\text{Pd}$  seeds (bottom panel). The 80 Gy isodose line was chosen as the prescription dose for the implant. Figure 6 plots the BED calculated at 19 different spatial locations on the isodose prescription line for several potential doubling times. The BED, dependent on the relative dose contribution by the  $^{103}\text{Pd}$  and  $^{125}\text{I}$  seeds, is different at different locations on the same isodose line. It demonstrates that the isodose prescription is inadequate for implants containing seeds of different half-lives. Clinically, if the dose prescription were established from existing implant experience that uses  $^{125}\text{I}$  seeds only, mixing  $^{103}\text{Pd}$  seeds with  $^{125}\text{I}$  seeds would increase the effective cell kill for the same prescribed dose. On the other hand, if the dose prescription were established from implant experience of using  $^{103}\text{Pd}$  seeds alone, mixing  $^{125}\text{I}$  seeds with  $^{103}\text{Pd}$  seeds in the

same implant would create radiobiologically "cold" spots (an increase in cell survival from the existing clinical experience) at locations where a major portion of the dose is contributed by the  $^{125}\text{I}$  seeds. These "cold" spots can become significant for fast growing tumors. The magnitude and spatial location of the "cold" spots can vary throughout the implant volume.

## DISCUSSION

As shown in the previous sections, new tools are needed for a meaningful implant evaluation when radionuclides of different half-life are used in the same implant. The generalized BED formula derived from Dale's work (11, 12) provides a tool to examine the interplay of the complex temporal dose delivery pattern in such an implant with the underlying radiobiologic processes. The calculation performed in this work suggests that the BED is always larger when the dose is delivered by  $^{103}\text{Pd}$  seeds compared with that by  $^{125}\text{I}$  seeds for any given sublethal damage repair and cell proliferation rates as long as the total dose is the same. Because the RBE arising from different linear energy transfer (22), secondary electrons generated by  $^{125}\text{I}$  and  $^{103}\text{Pd}$  photons, is not dealt with in this paper, the above conclusion is due purely to the difference in decay half-lives. Because the initial dose rate is always greater when using a radionuclide with shorter half-life, the conclusion drawn from the BED calculation is consistent with the dose rate effect (in the absence of cell cycle effect) observed over the years for protracted dose delivery (10, 23), albeit the dose rate is now

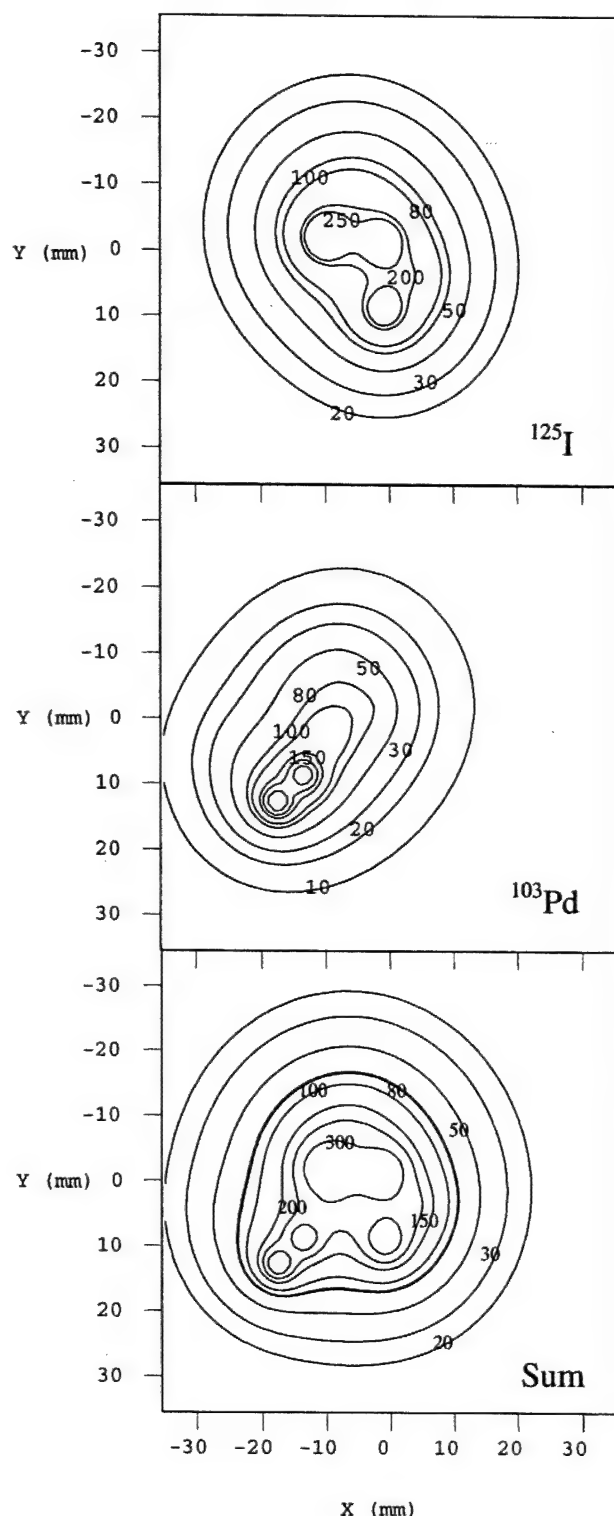


Fig. 5. Dose distribution on the  $x$ - $y$  plane for a head-and-neck implant using  $^{125}\text{I}$  and  $^{103}\text{Pd}$  seeds:  $^{125}\text{I}$  seeds alone (top),  $^{103}\text{Pd}$  seeds alone (middle), and from the actual implant with mixed seeds (bottom). The 80 Gy isodose line on the bottom panel was chosen as the clinical prescription isodose.

time-dependent in the permanent implants. Parenthetically, *in vitro* measurements have shown that the RBE for  $^{103}\text{Pd}$  is greater than that for  $^{125}\text{I}$  (22). If the RBE of  $^{103}\text{Pd}$  and  $^{125}\text{I}$

were taken into account in the model calculation, the observations made in this article would have been further reinforced.

Although the general conclusions drawn from the model calculation conform to common intuition, it should be emphasized that the quantitative numbers of BED should always be viewed in the context of the limitations inherent in the models. Many other factors that affect the radiobiologic responses of human tissues, such as the cell cycle effects (24), radiation-induced apoptosis (25, 26), and tissue architecture, were not considered in the current model. Even then, for the calculated BED to be clinically meaningful, one would have to know the patient-specific tumor potential doubling time, sublethal damage repair half-time, and other required model parameters. Given the simplistic nature of the biologic model and the lack of reliable means of determining the patient-specific model parameters at present, it would be inappropriate to treat the calculated BED as a quantitative predictor of the clinical outcome for a patient implant. Taking the current model as an example, the relative uncertainty in the calculated BED is determined by the relative uncertainty of each model parameter:

$$\frac{\Delta \text{BED}}{\text{BED}} = A \frac{\Delta \alpha}{\alpha} + B \frac{\Delta(\alpha/\beta)}{(\alpha/\beta)} + A \frac{\Delta T_p}{T_p} + C \frac{\Delta \mu}{\mu} \quad (9)$$

where the coefficients  $A$ ,  $B$ , and  $C$  are given by

$$A \equiv \frac{0.693 T_{\text{eff}} / T_p}{D(T_{\text{eff}}) RE - 0.693 T_{\text{eff}} / T_p}, \quad (10a)$$

$$B \equiv \frac{D(T_{\text{eff}})(1 - RE)}{D(T_{\text{eff}}) RE - 0.693 T_{\text{eff}} / T_p}, \quad (10b)$$

$$C \equiv \frac{D(T_{\text{eff}}) \mu \frac{\partial RE}{\partial \mu}}{D(T_{\text{eff}}) RE - 0.693 T_{\text{eff}} / T_p}. \quad (10c)$$

These coefficients determine the sensitivity of the calculated BED to the relative uncertainties that may incur in determining each model parameter. Because  $A$ ,  $B$ , and  $C$  are functions of the model parameters  $\{\alpha, \alpha/\beta, T_p, \mu\}$ , the influence of the relative uncertainty of a given model parameter on the calculated BED, in fact, depends on the characteristics of the tumor being studied. For example, the relative uncertainty associated with the potential tumor doubling time has a negligible effect on slowly growing tumors (i.e.,  $A \rightarrow 0$ , for  $T_p \rightarrow \infty$ ) but can be appreciable on fast growing tumors. Similarly, relative uncertainty incurred in determining  $\alpha/\beta$  would have less effect on tumors with larger  $\alpha/\beta$  than on tumors with small  $\alpha/\beta$ . For the repair time constant, however, BED is insensitive to  $\Delta \mu / \mu$  when repair is extremely slow or fast and is most sensitive at intermediate repair kinetics (see coefficient  $C$  and Fig. 3). Therefore, the numerical values of the calculated BED can not and should not be taken as a quantitative indicator of the

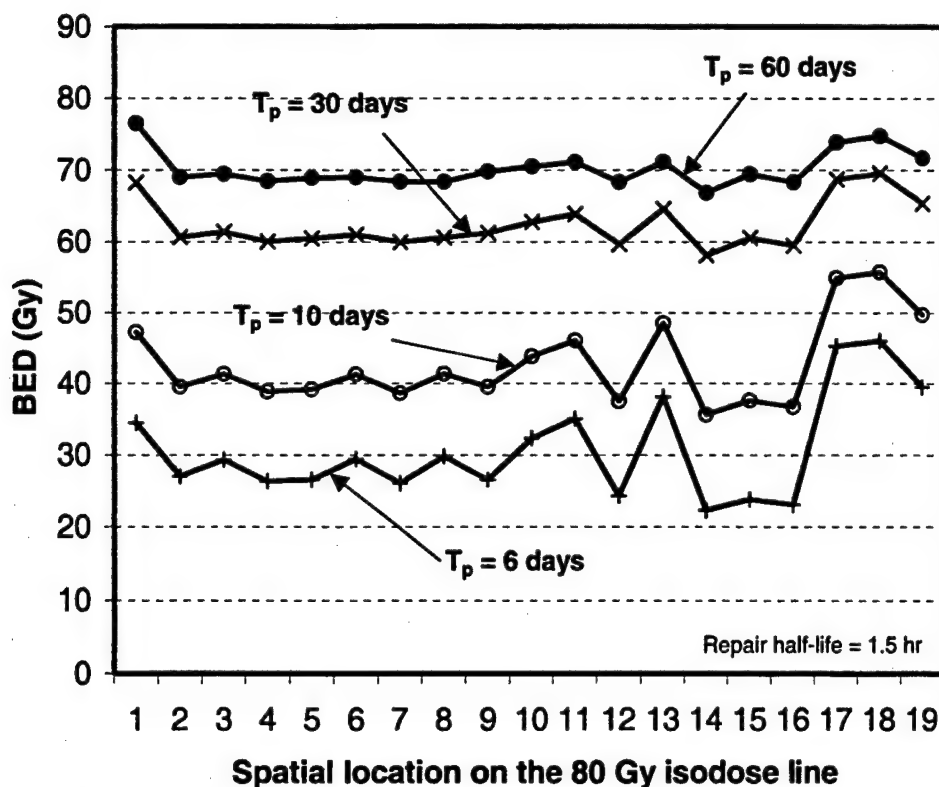


Fig. 6. BED at 19 spatial locations along the 80 Gy prescription isodose line for the head-and-neck implant with  $^{125}\text{I}$  and  $^{103}\text{Pd}$  seeds for various tumor potential doubling times. A sublethal damage repair half-life of 1.5 h and a  $\alpha/\beta$  of 10 for tumor were used in the calculation.

clinical outcome of a given implant at present. Nonetheless, the BED can be useful in comparing the relative merits of different physical implant strategies in a given implant by using a consistent set of radiobiologic model parameters. It is on this premise that we regard the BED formula as a useful tool for implant evaluation.

Many interesting issues arising from mixing seeds of different half-lives in the same implant can be examined using the generalized BED. For example, as mentioned in the "Introduction," it is interesting to examine whether a net gain in local control can be achieved by implanting both  $^{125}\text{I}$  and  $^{103}\text{Pd}$  seeds in tumors that may contain both fast and slow growing cells. If the answer were affirmative, there may exist an optimal mixture for a known proportion of slow and fast growing cells. Also, the cells in the surrounding normal structures are known to exhibit very slow proliferation rates. Because radiobiologic "cold" spots are desirable in the normal structures, it would be interesting to find out if the spatial location of the seeds of different half-lives can be so arranged such that the cell survival in the nearby normal structures is maximized, without compromising the effective cell kill in the tumor volume. Detailed discussion of these and other issues is, unfortunately, outside the scope of this paper, and they will be dealt with elsewhere.

The clinical implant used for examining the appropriateness of isodose prescription in implants containing seeds of different half-lives is one of two such implants ever per-

formed. Because the dose prescription for the implant was based on the experience of using  $^{125}\text{I}$  seeds alone, the effective cell kill in the clinical implant is expected to be greater than those implants using  $^{125}\text{I}$  seeds alone. These two implants, however, cannot be used to answer a more general question, i.e., whether the expected increase in cell kill will translate to increased local control when compared with existing implant experience using  $^{125}\text{I}$  alone. Such a question can only be answered through systematic clinical trials on a large number of patients with known clinical presentations.

For a complete evaluation of an implant containing seeds of different half-lives, BED over the entire volume of interest should be examined because the total dose and initial dose rate are inherently inhomogeneous. With the advance of medical imaging modalities and image-based treatment planning (27), we hope that three-dimensional tissue structures can be identified more accurately and that a 3D distribution of BED can be calculated with confidence (28). With the BED distribution, radiobiologically significant "cold" spots, due either to "cold" spots in total dose or to the "cold" spots in dose rate, can be identified during the planning of an interstitial seed implant.

## CONCLUSIONS

A generalized Dale equation for BED is presented for interstitial implants containing a mixture of radionuclides

with different half-lives. The generalized BED provides a tool for evaluating the radiobiologic effects of mixing different types of radionuclides in the same implant. Model calculation performed in this paper suggests that adding the  $^{103}\text{Pd}$  to the  $^{125}\text{I}$  implant would increase the effectiveness of

cell kill, whereas the opposite is not true if the dose prescription was based on the clinical experience established with the  $^{125}\text{I}$  implants. It is hoped that this work will stimulate further research interest in improving the radiobiologic modeling.

## REFERENCES

- Blasko JC, Grimm PD, Ragde H, Schumacher D. Implant therapy for localized prostate cancer. In: Ernstoff MS, Heaney JA, Peschel RE, editors. Prostate cancer. Cambridge, Massachusetts and Oxford, England: Blackwell Science; 1998. p. 137-155.
- Lefebvre JL, Coche-Dequeant B, Castelain B, Prevost B, Buisset E, Ton Van J. Interstitial brachytherapy and early tongue squamous cell carcinoma management. *Head Neck* 1990;12:232-236.
- Son YH, Sasaki CT. Nonsurgical alternative therapy for bulky advanced head and neck tumors. *Arch Otolaryngol Head Neck Surg* 1995;121:991-993.
- Vikram B, Mishra S. Permanent iodine-125 implants in post-operative radiotherapy for head and neck cancer with positive surgical margins. *Head Neck* 1994;16:155-157.
- Wilson LD, Chung JY, Haffty BG, Cahow EC, Sasaki CT, Son YH. Intraoperative brachytherapy, laryngopharyngoesophagectomy, and gastric transposition for patients with recurrent hypopharyngeal and cervical esophageal carcinoma. *Laryngoscope* 1998;108:1504-1508.
- Nath R. New directions in radionuclide sources for brachytherapy. *Semin Radiat Oncol* 1993;3:278-289.
- Kinsey RR. The NuDat Program for Nuclear Data on the Web. National Nuclear Data Center, Brookhaven National Laboratory. (<http://www.nndc.bnl.gov/nndc/nudat/>). Database last updated August 12, 1999.
- Hilaris BS, ed. Handbook of interstitial brachytherapy. Acton, MA: Publishing Science Group; 1975.
- Ling CC. Permanent implants using Au-198, Pd-103, and I-125: Radiobiological considerations based on the linear quadratic model. *Int J Radiat Oncol Biol Phys* 1992;23:81-87.
- Hall EJ. Radiobiology for the radiologist. 4th ed. Philadelphia: Lippincott; 1994.
- Dale RG. The application of the linear-quadratic dose-effect equation to fractionated and protracted radiotherapy. *Br J Radiol* 1985;58:515-528.
- Dale RG. Radiobiological assessment of permanent implants using tumor repopulation factors in the linear-quadratic model. *Br J Radiol* 1989;62:241-244.
- Thames HD. An "incomplete-repair" model for survival after fractionated and continuous irradiation. *Int J Radiat Biol* 1985;47:319-339.
- Fowler JF. The linear-quadratic formula and progress in fractionated radiotherapy. *Br J Radiol* 1989;62:679-694.
- Barendsen GW. Dose fractionation, dose rate and iso-effect relationships for normal tissue response. *Int J Radiat Oncol Biol Phys* 1982;8:1981-1997.
- Ling CC, Roy J, Sahoo N, Wallner K, Anderson L. Quantifying the effect of dose inhomogeneity in brachytherapy: Application to permanent prostatic implant with  $^{125}\text{I}$  seeds. *Int J Radiat Oncol Biol Phys* 1994;28:971-978.
- Nath R, Anderson LL, Luxton G, Weaver KA, Williamson JF, Meigooni AS. Dosimetry of interstitial brachytherapy sources: Recommendations of the AAPM radiation therapy committee task group 43. *Med Phys* 1995;22:209-234.
- Dale RG, Jones B. The clinical radiobiology of brachytherapy. *Br J Radiol* 1998;71:465-483.
- Orton CG. Update on time-dose models. In: Purdy JA, editor. Advances in radiation oncology physics dosimetry, treatment planning, and brachytherapy. : American Institute of Physics; 1992. Woodbury, NY: p. 374-389.
- Haustermans KMG, Hofland I, Van Poppel H, et al. Cell kinetic measurements in prostate cancer. *Int J Radiat Oncol Biol Phys* 1997;37:1067-1070.
- Dale RG, Coles IP, Deehan C, O'Donoghue J. The calculation of integrated biological responses in brachytherapy. *Int J Radiat Oncol Biol Phys* 1997;38:633-642.
- Ling CC, Li WX, Anderson LL. The relative biological effectiveness of I-125 and Pd-103. *Int J Radiat Oncol Biol Phys* 1995;32:373-378.
- Hall EJ. Radiation dose rate: A factor of importance in radiobiology and radiotherapy. *Br J Radiol* 1972;45:81-97.
- Knox SJ, Sutherland W, Goris MC. Correlation of tumour sensitivity to low dose rate irradiation G2/M phase block and other radiobiological parameters. *Radiat Res* 1993;135:24-31.
- Ling CC, Chen CH, Fuks Z. An equation for the dose response of radiation-induced apoptosis: Possible incorporation with the LQ model. *Radiation Oncol* 1994;33:17-22.
- Ling CC, Chen CH, Li WX. Apoptosis induced at different dose rates: Implication for the shoulder region of cell survival curves. *Radiation Oncol* 1994;32:129-136.
- Martel MK, Narayana V. Brachytherapy for the next century: Use of image-based treatment planning. *Radiat Res* 1998;150: S178-188.
- Lee SP, Len MY, Smathers JB, McBride WH, Parker RG, Withers HR. Biologically effective dose distribution based on the linear quadratic model and its clinical relevance. *Int J Radiat Oncol Biol Phys* 1995;33:375-389.

## APPENDIX

Equation 5 can easily be derived following the work of Dale (11, 12) for implants containing a single type of radionuclide. The reader is referred to Dale's original articles (11, 12) for the detailed steps and the rationale underlying the derivation. The main derivation steps are outlined below.

Dale has invoked the assumption that a lethal radiation damage is caused by the damage of two critical targets in a cell. When the two critical targets are damaged simulta-

neously by a radiation event, the resulting lethal damage is termed type A damage. When a radiation event damages only one critical target, the cell is considered sublethally damaged, which is repairable. In the latter case, a lethal damage results when the second critical target is damaged before the existing sublethal damage is fully repaired. This type of lethal damage is termed type B damage. Type A damage is always proportional to the total delivered dose irrespective of dose rate, whereas the type B damage is dose

rate dependent because the independently damaged targets may be repaired over time. The overall radiation-induced cell inactivation is therefore proportional to the sum of type A and type B damages. The main goal in deriving the BED is to determine the total probability of type A and type B damages over the time period of a given dose delivery.

For an implant with a mixture of radionuclides, the instantaneous dose rate to a point of interest at time  $t$  after the implant is given by Eq. 2 in the main text as

$$\dot{D}(t) = \sum_{i=1}^M \dot{D}_{0i} e^{-\lambda_i t} \quad (\text{A1})$$

where the summation is over different types of radionuclides used in the implant. Using this expression for instantaneous dose rate, the derivation for BED follows almost exactly the same steps outlined in the appendix of Dale's article (11, 12).

The type A damage is proportional to the dose delivered. Therefore, the total type A damage accumulated over a period of time  $T$  after seed implantation is given by

$$\text{Total type - A damage} = \alpha \sum_i \frac{\dot{D}_{0i}}{\lambda_i} (1 - e^{-\lambda_i T}) \quad (\text{A2})$$

The type B damage is determined by the joint probability of two targets being damaged at different times by two different radiation events. By assuming the sublethal damage repairs exponentially with time, the total type B damage accumulated over the same period of time  $T$  after seed implantation can be determined.

$$\begin{aligned} \text{Total Type - B damage} &= 2\beta \sum_i \sum_j \frac{\dot{D}_{0i} \dot{D}_{0j}}{\mu - \lambda_i} \\ &\times \left\{ \frac{1}{\lambda_i + \lambda_j} (1 - e^{-(\lambda_i + \lambda_j)T}) - \frac{1}{\lambda_j + \mu} (1 - e^{-(\mu + \lambda_j)T}) \right\} \quad (\text{A3}) \end{aligned}$$

In the above expressions,  $\alpha$  and  $\beta$  are the linear and quadratic coefficients, respectively, of the linear-quadratic cell inactivation model.  $\mu$  is the repair time constant that characterizes the rate of sublethal damage repair.

With Eqs. A2 and A3, the ratio of total lethal damage to the type A lethal damage alone, termed relative effectiveness by Dale, can be determined as

$$\begin{aligned} \text{RE} &= 1 + \frac{\text{Total type - B damage}}{\text{Total type - A damage}} = 1 + 2 \left( \frac{\beta}{\alpha} \right) \\ &\frac{\sum_i \sum_j \frac{\dot{D}_{0i} \dot{D}_{0j}}{\mu - \lambda_i} \left\{ \frac{1}{\lambda_i + \lambda_j} (1 - e^{-(\lambda_i + \lambda_j)T}) - \frac{1}{\lambda_j + \mu} (1 - e^{-(\mu + \lambda_j)T}) \right\}}{\sum_i \frac{\dot{D}_{0i}}{\lambda_i} (1 - e^{-\lambda_i T})} \quad (\text{A4}) \end{aligned}$$

Equation A4 is the main result of this derivation. The BED for an implant with a mixture of radionuclides is therefore given by

$$\text{BED} = \sum_i \frac{\dot{D}_{0i}}{\lambda_i} (1 - e^{-\lambda_i T_{\text{eff}}}) \text{RE} - \frac{0.693}{\alpha T_p} T_{\text{eff}} \quad (\text{A5})$$

where  $T_p$  is the tumor potential doubling time. Note that  $T_{\text{eff}}$  is the effective treatment time at which the tumor cell-proliferation rate exceeds the tumor cell-inactivation rate caused by the instantaneous dose rate at that time.

As expected, for implants with a single type of radionuclide,  $i = j = 1$ , and Eqs. A4 and A5 reduce to Dale's original equation

$$\begin{aligned} \text{RE} &= 1 + 2 \left( \frac{\beta}{\alpha} \right) \dot{D}_0 \frac{\lambda}{\mu - \lambda} \frac{1}{(1 - e^{-\lambda T})} \\ &\times \left\{ \frac{1}{2\lambda} (1 - e^{-2\lambda T}) - \frac{1}{\lambda + \mu} (1 - e^{-(\mu + \lambda)T}) \right\} \quad (\text{A6}) \end{aligned}$$

**Dose rate dependence of the relative biological effectiveness of  $^{103}\text{Pd}$  for Continuous Low Dose Rate Irradiation of BA1112 Rhabdomyosarcoma Cells in vitro relative to Acute Exposures**

Ravinder Nath, Paul Bongiorno, Zhe Chen, Jillian Gragnano, and Sara Rockwell

Department of Therapeutic Radiology, Yale University School of Medicine, 333 Cedar Street, New Haven, Connecticut 06510

(Submitted to International Journal of Radiation Biology on )

Supported in part by DOD grant no. DAMD 17-00-1-0052, awarded by the Department of Army

## Abstract

Relative biological effectiveness (RBE) of continuous low dose rate irradiation using  $^{103}\text{Pd}$  sources was measured relative to acute exposures using an x-ray beam which was simulated to generate a nearly monoenergetic photon energy similar to that of  $^{103}\text{Pd}$ . The survival curves were fitted to the linear-quadratic model for continuous low dose rate irradiation. A profound dose rate effect is observed at the low dose rates in the range of 6.8 to 14.4 cGy/hr that are typical of permanent interstitial brachytherapy. At a survival level of 0.01, the RBE of CLDRI at 6.8 and 14.4 cGy/hr using  $^{103}\text{Pd}$  sources relative acute exposures at a dose rate of 333 cGy/hr from a simulated x-ray beam, is reduced by a factor of 3 and 2, respectively.



## Methods and Materials

### BA1112 cells

Animals were implanted with transplanted BA1112 rhabdomyosarcomas by the inoculation of 7500 tumor cells, suspended in 0.05 ml of sterile cell culture medium, into a subcutaneous site on the head. The tumors were allowed to grow for 3 weeks, to an experimental volume of approximately 100-200 mm<sup>3</sup>. The animals chosen for the in vitro irradiations of the BA1112 sarcoma cells were euthanized by anesthetic overdose and the tumor was removed using aseptic techniques. The tumor was chopped into a fine mash with a sterile blade, and the tumor pieces added to a trypsin solution and stirred at 37°C for 15 minutes. The suspension is now filtered to remove pieces of contaminants and centrifuged at 400G for 10 minutes, then re-suspended in 10ml of DMEM culture media. This single-cell suspension of tumor cells will be counted, and assayed for viability using the same colony formation assay used for cells in cultures and seeded into experimental dishes at cell concentrations of  $5 \times 10^5$  to  $1.5 \times 10^6$ . The dishes are put into a 37°C incubator with 95% air/5% CO<sub>2</sub>. These cells are allowed to attach to the petri dishes (60mm), and begin to divide, at least 48 hrs, before dishes are used for inv vitro irradiations.

### In vitro irradiation technique for acute irradiation

The radiobiological response of the cells under acute exposure condition was studied using a simulated x-ray beams with average energies equivalent to that emitted <sup>103</sup>Pd (20 – 22.7 keV with an average of 20.5 keV) generated by an orthovoltage unit (Pantek, CT). The simulated beams not only have the average energies similar to that given by the radioactive isotopes but also have a narrow photon energy spectrum. The narrow photon energy spectrum was achieved by optimizing the tube voltage (which determines the upper limit of the photon energy) and by added filtration (which filters out the low-energy Bremsstrahlung photons), following the work of Muench et al<sup>5</sup>.

The beam quality of the simulated beam was monitored while the tube voltage and the added filtration were optimized. The half-value-layer of the simulated beam was measured using aluminum filters (with thickness of 0.1 to 1.0 mm) from Nuclear Associates under narrow beam condition. A narrow circular beam, with a diameter of 6 cm at source to chamber distance (SCD) of 50 cm, was produced a homemade lead collimator mounted to DXT 300's accessory mount. The aluminum sheets added to the beam for the HVL measurement were taped to the bottom of the lead collimator. An air-equivalent Spokas chamber (Exradin, Model No: A1 (0.5 ml, AE plastic)) was used to measure the ionization at the SCD of 50 cm in air. Due the energy dependence of the chamber at the low energies, the measured ionization were converted to corresponding exposure and the HVL is then determined from the relative exposure as a function of aluminum filter thickness. Figure 1 plots the relative exposure as a function of filter thickness obtained for the HVL measurement. The measured HVL was then used to determine the energy of an equivalent mono-energetic photon beam. The HVL as a



function of mono-energetic photon beam energy for aluminum is taken from Johns and Cunningham<sup>6</sup>. The optimized  $^{103}\text{Pd}$  x-ray beam has a HVL of 0.84 mm Aluminum and equivalent mono-energetic photon energy of 20.7 keV (average energy from  $^{103}\text{Pd}$  sources is 20.9 keV). Table I summarizes the setting for the simulated  $^{103}\text{Pd}$  beam used for acute in vitro cell survival studies.

Radiation output for the simulated beam was determined by the measured average dose to tissue culture medium in the petri dish using Fricke dosimetry. It was crosschecked using the air-equivalent Spokas chamber and a calibrated parallel-plate soft energy chamber. Since the Fricke dosimetry was carried out using the same petri dish with similar amount of solution as used for in vitro irradiation, its measured output was used in computing the dose for this experiment. The dose rate to the petri dish was determined to be 33.3 Gy/hr.

### **In vitro irradiation technique for CLDRI**

A specially designed  $^{103}\text{Pd}$  source irradiators made of polystyrene with a central hole for placing the petri dishes on top of the sources, with or without some polystyrene spacers between the sources and the tissue culture dishes was built in our lab (Fig. 1). The irradiator consists of a 20.3 x 20.3 x 10.2 cm polystyrene phantom with a 10.2 cm diameter centered hole containing a polystyrene disk loaded with  $^{103}\text{Pd}$  sources. The irradiator was loaded with 26  $^{103}\text{Pd}$  sources (model 200; Theragenics Corp., Norcross, Atlanta), each with an initial activity of xx mCi. The sources are arranged in a circle with a diameter of 6 cm, and two sources are placed next to each other at the center of the circle. These sources were contained in a 1.25 cm thick, 10 cm diameter polystyrene disc. Different dose rates spanning the range from 6 to 13 cGy/hr were obtained by varying the thickness of the polystyrene spacers. The  $^{103}\text{Pd}$  irradiator was placed in a 37°C water-jacketed incubator and surrounded in lead foil of 1 mm thickness to shield the photons.

The dose to cells in the monolayers was determined from the measured average dose to tissue culture medium in the petri dish using Fricke dosimetry, with a calculated correction for interface effects due to photoelectric effect in the tissue culture dishes []. The uniformity of dose rate across the petri dish was verified by three independent means: LiF thermoluminescent dosimetry, film dosimetry and dose calculations by a computerized treatment planning package (Theraplan). In all cases, the dose uniformity across the petri dish was better than  $\pm 5\%$ .

### **Cytotoxicity studies**

All experiments were performed using cell monolayers that were prepared by plating cells, suspended from exponentially growing stock cultures, into 60-mm diameter Falcon tissue culture dishes. The cells were incubated for 18 hr prior to irradiation, to allow them to attach and to progress into exponential growth. Once the cells were in exponential growth, the growth medium was removed and replaced by fresh growth medium just before the beginning of the irradiations, which lasted 1 to 60 hr in CLDRI.

Cells were maintained in a humidified 95% air-5% CO<sub>2</sub> environment at 37°C during irradiations, as well as during control conditions. After irradiation, the cells were washed with Hanks' balanced salt solution, trypsinized, and counted using a Coulter counter, equipped with a Channelizer to allow assessment of and correction for any changes in cell size. Cells were plated for colony formation in at least four dishes per data point and were allowed to grow in a humidified 95% air-5% CO<sub>2</sub> environment at 37°C for 10 days. The colonies were then fixed, stained, and counted. Experiments were planned to obtain approximately 120 colonies in each dish, by adjusting the number of cells plated per dish appropriately. Cytotoxicity was characterized using cell survival fraction, which is a ratio of plating efficiencies of the treated cells relative to those of unirradiated cells under control conditions. In these experiments, however, the numbers of cells in cultures treated with CLDRI were significantly lower than the numbers of cells in control cultures, even though the same numbers of cells were used to initiate the cultures, because of reduced rates of cell division in the irradiated cultures and because some cells died during the prolonged irradiations. The surviving fractions were therefore corrected to account for the deficit in cell number in the irradiated cultures, using the formula:

$$S = \frac{P_{\text{exptl}}}{P_{\text{control}}} G \frac{C_{\text{exptl}}}{C_{\text{control}}} \quad (1)$$

where

$P_{\text{exptl}}$	= plating efficiency of the experimental sample;
$P_{\text{control}}$	= plating efficiency of the control sample;
$C_{\text{exptl}}$	= number of cells harvested from the experimental sample at the end of irradiation time;
$C_{\text{control}}$	= number of cells harvested from the control sample assayed at the end of irradiation time (without irradiation).

Plating efficiencies (colonies formed/cells plated) for untreated cells were approximately 90% in the experiments reported here.

## RESULTS AND DISCUSSIONS

The cell loss in irradiated cultures, described in the materials and methods section, was calculated as  $(1 - C_{\text{exptl}}/C_{\text{control}})$  for all dose rates studied here (Figure 3). These data were fitted with straight lines with no intercepts. The slopes of these lines, i.e. the rates of cell loss during irradiation, increased monotonically with increasing dose rate for both cell lines and both radioisotopes. The slopes were similar for the two cell lines. This confirms that the cell loss is basically a dose rate effect primarily related to the length of irradiation period.

Figure 4 plots the cell survival curves for the BA1112 cells irradiated by  $^{103}\text{Pd}$  at different dose rates. The lines are fit to the measured data using the linear-quadratic (LQ) survival model. At low dose rate, the survival data were fitted only to the linear term of the LQ model because the quadratic term did not significantly improve the goodness of the fit. If the fit to the low dose rate survival data can be extrapolated to higher dose (not guaranteed), the relative biological effectiveness (RBE) of the CLDRI can be compared to the acute irradiation using the simulated  $^{103}\text{Pd}$  beam. At the survival level of 0.01, the RBE of CLDRI at dose rates of 14.4 cGy/hr and 6.8 cGy/hr was found to be 0.49 and 0.31, respectively. The relative effectiveness as compared to acute irradiation was reduced by a factor of 2 and 3 for the CLDRI dose rates of 14.4 cGy/hr and 6.8 cGy/hr, respectively.

(Model calculation will be added later)

## Conclusion

Relative biological effectiveness of continuous low dose rate irradiation using  $^{103}\text{Pd}$  sources has been measured relative to acute exposures using an x-ray beam which was simulated to generate a nearly monoenergetic photon energy similar to that of  $^{103}\text{Pd}$ . A profound dose rate effect is observed at the low dose rates in the range of 6.8 to 14.4 cGy/hr that are typical of permanent interstitial brachytherapy. At a survival level of 0.01, the RBE of CLDRI at 6.8 and 14.4 cGy/hr using  $^{103}\text{Pd}$  sources is reduced by a factor of 3 and 2, respectively, relative acute exposures at a dose rate of 333 cGy/hr from a simulated x-ray beam.

**Table I. Beam characteristics of simulated  $^{103}\text{Pd}$  x-ray beams**

Beam	kV	mA	Added Filter (mm AL)	Beam HVL (mm AL)	Energy Homogeneity (%)	Equivalent Energy (keV)	$\langle E \rangle$ from isotope (keV)
<b>Pd-103 Equivalent</b>	29	25	1.826	0.84	88.6	20.7	20.7

**Table II RBE of CLDRI using  $^{103}\text{Pd}$  sources**

Radiation Source	Dose Rate (Gy/hr)	RBE relative to simulated x-rays
Pd-103	0.068	0.49
Pd-103	0.144	0.31
Simulated x-rays	33.3	1

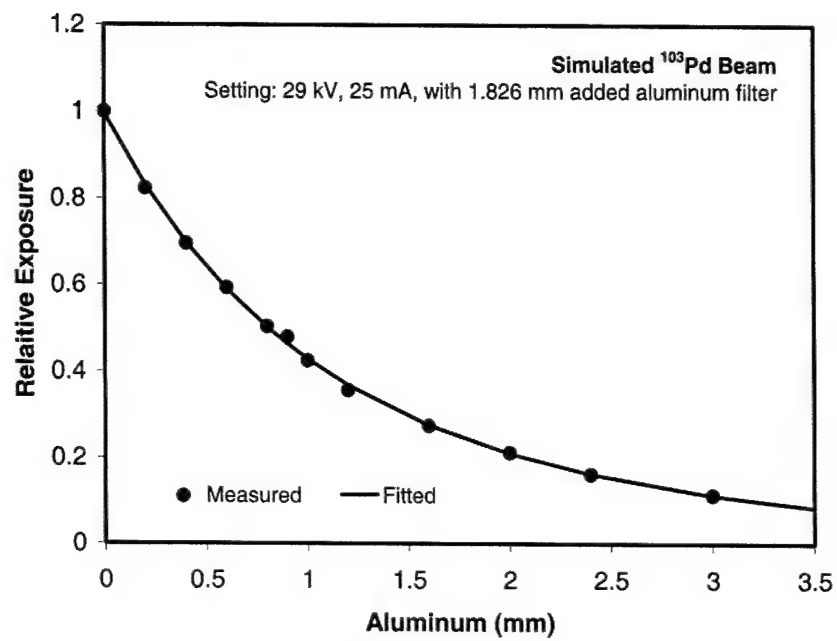


Figure 1

Figure 2.  $^{103}\text{Pd}$  irradiator

Figure 3. Cell loss curves

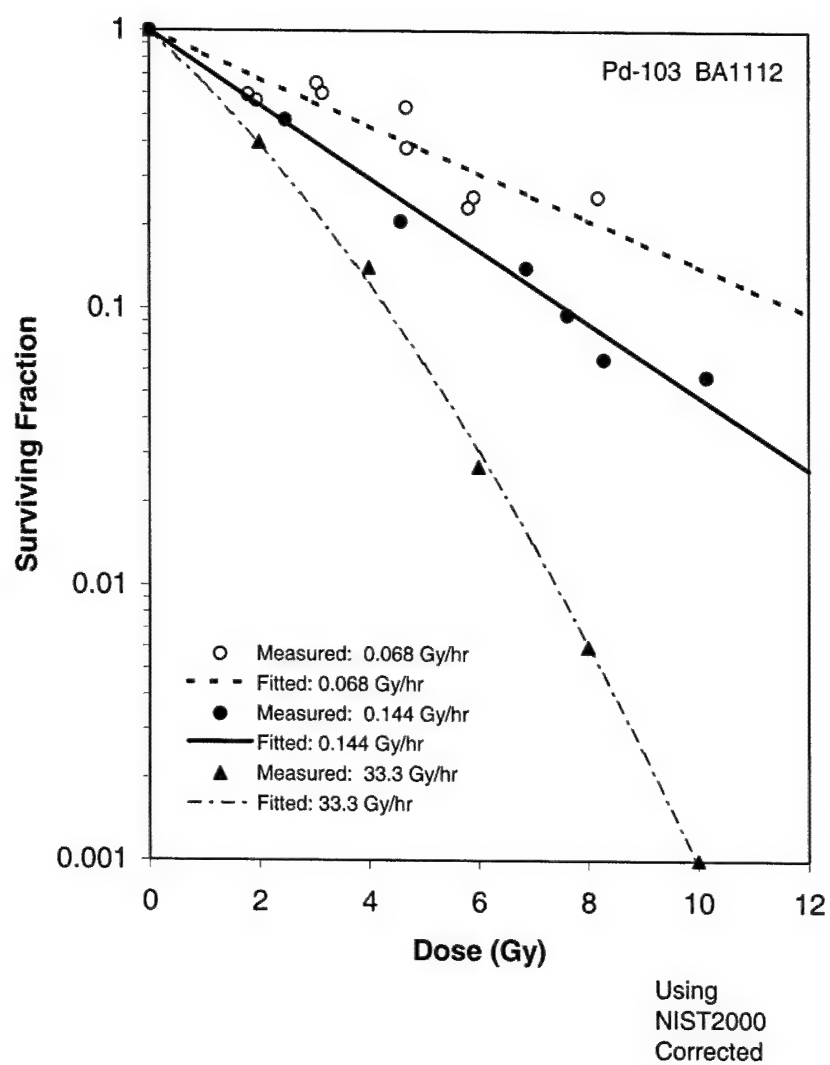


Figure 4

**APPENDIX III**  
**Radiobiological parameters for the CCL-16 cell line**

1. Tumor growth

a. In vitro tumor cell growth

**Method:**

**Results:** Figure 1 plots the in vitro tumor cell growth as a function of time. The cell doubling time for tumor proliferation is estimated by fitting the cell growth to an exponential function. The  $T_{1/2}$  was found to be 13 hours (0.55 days) (file: CCL\_Growth.xls)

2. Sublethal damage repair time constant

a. Split dose experiments

**Method:** Split dose experiment was performed for CCL-16 cell line using the 250 kV x-rays. A total dose of 8 Gy was given. The survival fraction was measured as a function of time interval between two 4 Gy irradiation. The cells were kept at 22°C during the waiting interval to prevent proliferation. According to incomplete repair model we have,

$$\frac{\ln[S(t)/S(0)]}{\ln[S(\infty)/S(0)]} = 1 - e^{-\mu t}$$

where  $S(t)$  is the surviving fraction with split time interval  $t$  and  $\mu$  is the sub-lethal damage repair time constant.

**Results:** Figure 2 plots the measured survival and the curved fitted to the above equation. The repair half-time was found to be 13 minutes (file: ccl\_splitdose.xls).

3.  $\alpha$  and  $\beta$  for the linear-quadratic cell survival model

The parameters of  $\alpha$  and  $\beta$  for the CCL-16 cell line for  $^{125}\text{I}$ ,  $^{103}\text{Pd}$ , and 250 kV photons were determined from the survival curves obtained under acute exposure condition using simulated  $^{125}\text{I}$  and  $^{103}\text{Pd}$  x-ray beam on an orthovoltage unit. To obtain the  $\alpha$  and  $\beta$ , the acute survival curves for the simulated  $^{125}\text{I}$ ,  $^{103}\text{Pd}$ , and the 250 kV x-rays were fitted to the LQ cell survival equation. Two fitting procedures were used. In the first procedure, the  $\alpha/\beta$  ratio were kept the same for all three radiation beam qualities. The  $\alpha$  for each beam quality and  $\alpha/\beta$  were treated as fitting parameters in the global fit (Fig.3A). The second approach is similar to the first procedure except the  $\beta$  was regarded the same for all three beam qualities (Fig.3B). The fitted  $\alpha$  and  $\beta$  is given in the attached table. It should be noted that the relationship between the cell survival curve of 250 kV x-rays and those from  $^{125}\text{I}$  and  $^{103}\text{Pd}$  does not appear consistent with the general trend observed on the cell kill as a function of LET. Investigation on this observation is being conducted. Due

to this observed inconsistency, a global fit using only the  $^{125}\text{I}$  and  $^{103}\text{Pd}$  beams were also performed (Fig. 4A with fixed  $\alpha/\beta$  and Fig. 4B with fixed  $\beta$ ). The fitted parameters are listed in a separate table.

### Radiobiological Parameters Determined from Acute Exposure Experiments

Beam quality	Parameters for CCL-16				
	$\alpha$ (Gy <sup>-1</sup> )	$\beta$ (Gy <sup>-2</sup> )	$\alpha/\beta$ (Gy)	Tumor Doubling Time (day)	Sub-lethal Damage Repair Half-time (hr)
250 kV	0.17	0.037	4.7	0.55	0.21
$^{125}\text{I}$ equivalent	0.12	0.025	4.7	0.55	0.21
$^{103}\text{Pd}$ equivalent	0.16	0.033	4.7	0.55	0.21
250 kV	0.23	0.031	7.4	0.55	0.21
$^{125}\text{I}$ equivalent	0.07	0.031	2.1	0.55	0.21
$^{103}\text{Pd}$ equivalent	0.18	0.031	5.7	0.55	0.21

### Radiobiological Parameters Determined from Acute Exposure Experiments (using only $^{125}\text{I}$ and $^{103}\text{Pd}$ beams)

Beam quality	Parameters for CCL-16				
	$\alpha$ (Gy <sup>-1</sup> )	$\beta$ (Gy <sup>-2</sup> )	$\alpha/\beta$ (Gy)	Tumor Doubling Time (day)	Sub-lethal Damage Repair Half-time (hr)
$^{125}\text{I}$ equivalent	0.17	0.021	8.3	0.55	0.21
$^{103}\text{Pd}$ equivalent	0.22	0.027	8.3	0.55	0.21
$^{125}\text{I}$ equivalent	0.14	0.024	5.9	0.55	0.21
$^{103}\text{Pd}$ equivalent	0.25	0.024	10.6	0.55	0.21



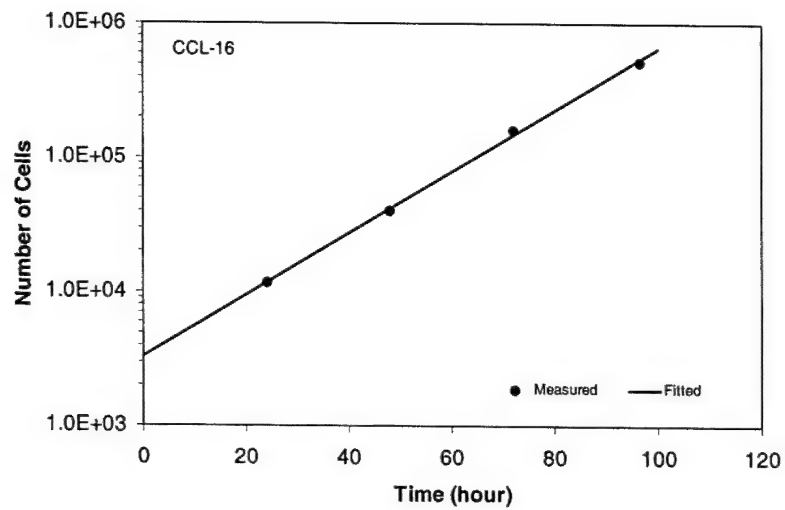


Figure 1

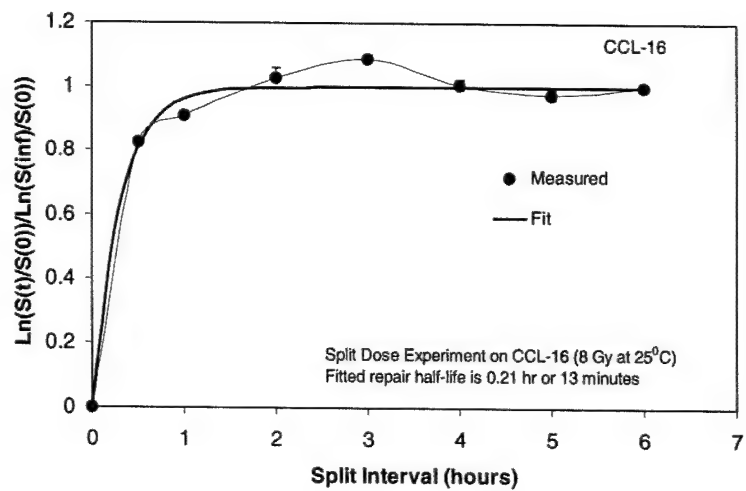


Figure 2

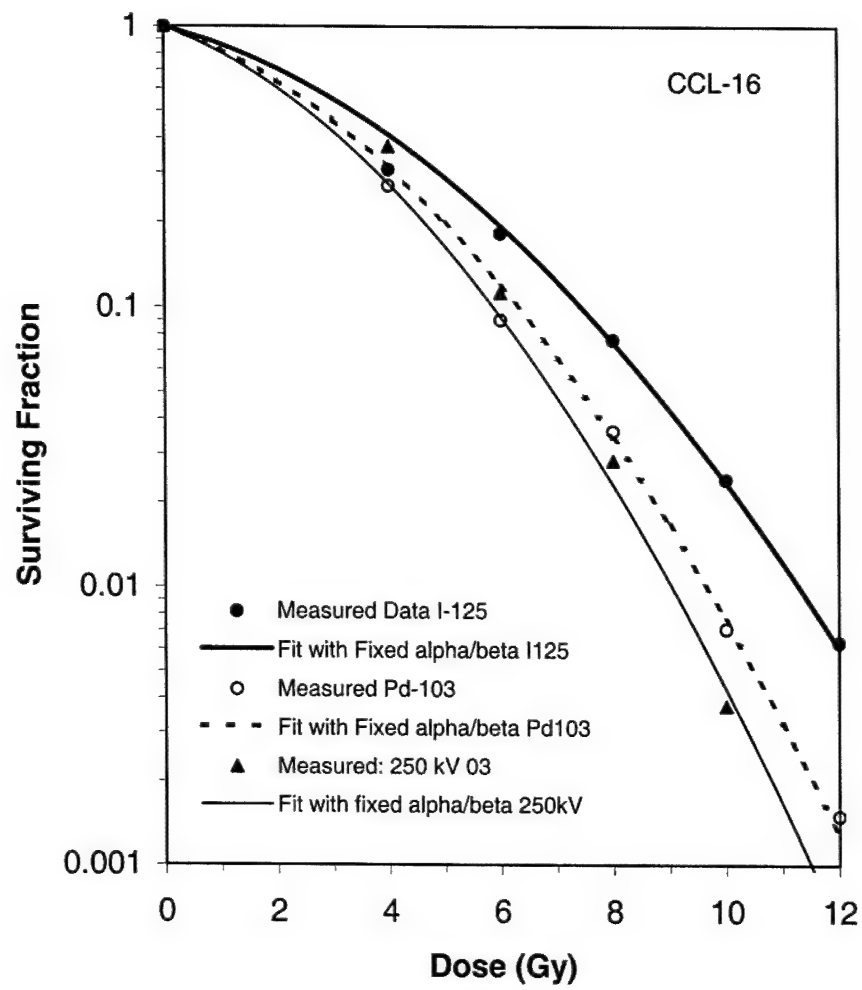


Figure 3A

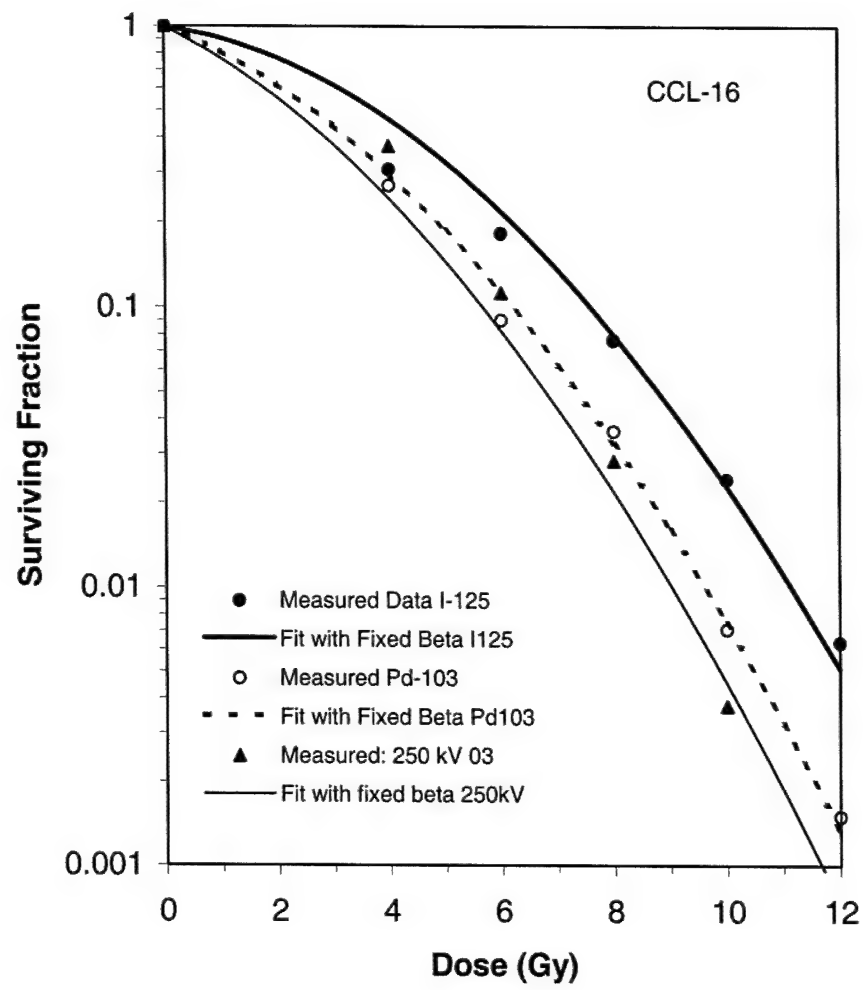


Figure 3B

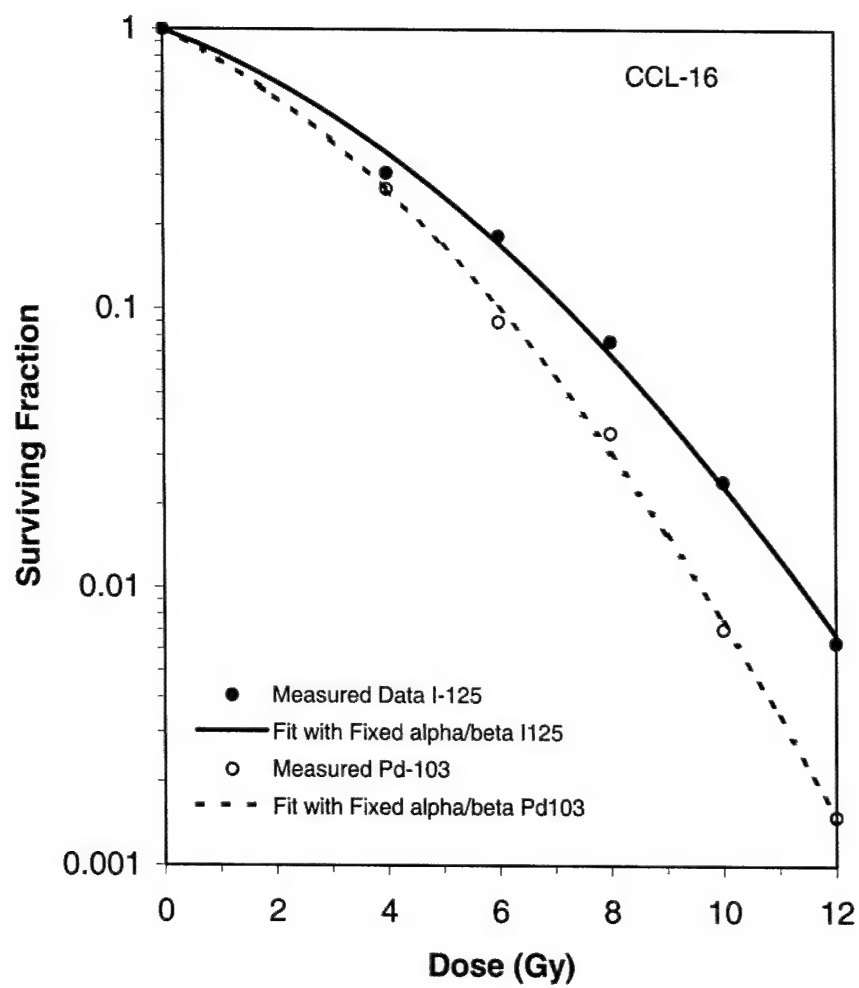


Figure 4A

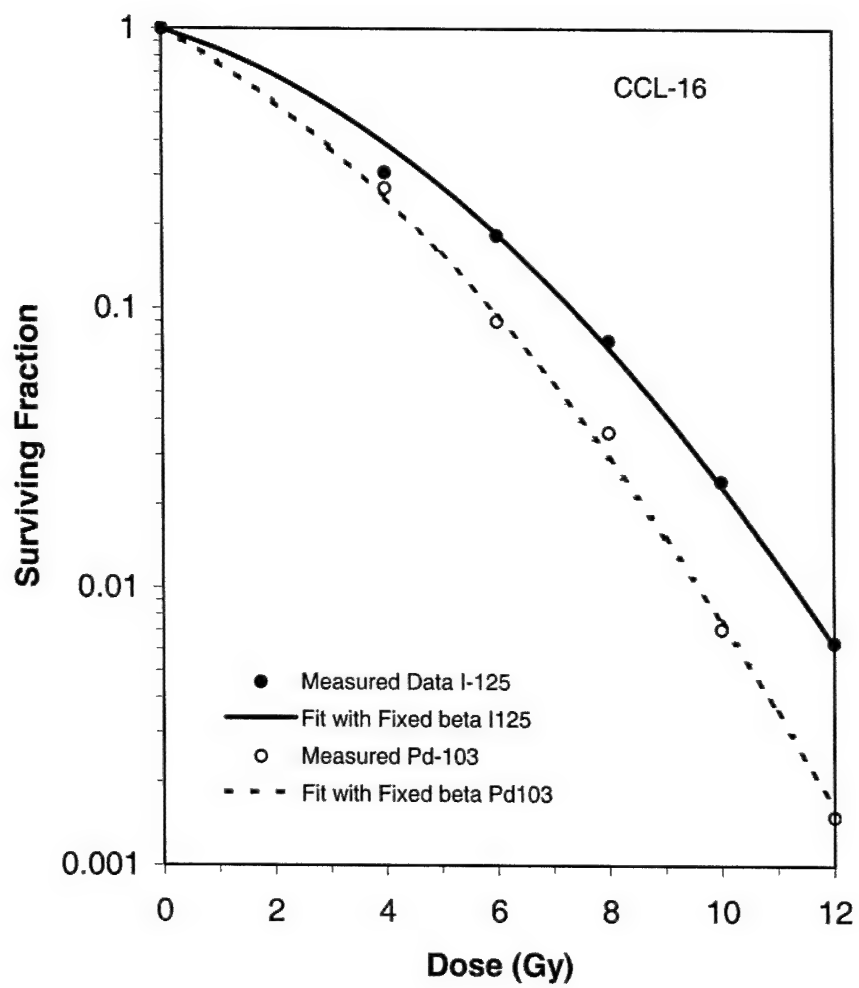


Figure 4B

**APPENDIX IV**  
**Radiobiological parameters of the BA1112 rhabdomyosarcomas**

1. Growth characteristics

a. In vitro cell growth

**Methods:** In vitro tumor cell growth rate was determined by examine the cell growth,  $\text{Ln}\{N(t)/N(0)\}$ , as a function of time.

**Results:** Figure 1 plots the measured  $\text{Ln}\{N(t)/N(0)\}$  as a function of time from four experiments. (Explanation of the cell number reduction at large times). The tumor cell doubling time in the exponential growth phase (between the elapsed time of 0 and 96 hours) was found to be 20 hours from least square fit. (file: growth curve invitro xc.xls)

b. In vivo tumor growth

**Methods:** Animals were implanted with transplanted BA1112 rhabdomyosarcomas by the inoculation of 7500 tumor cells, suspended in 0.05 ml of sterile cell culture medium, into a subcutaneous site on the head. An aseptic technique was used during the inoculation. The rats were anesthetized with xylazine/ketamine (0.005 mg/g and 0.075 mg/g, respectively) given IP, and a small area on the rats' head was shaved for the subcutaneous injection of tumor cells. The actual inoculation of tumor cells take approximately 3 minutes followed by the administering of Yohimbine (0.002 mg/g) IP to counteract the effects of the xylazine. The animal is awake and alert in approximately 20-30 minutes. The tumors were allowed to grow tumor volume were measured as a function of elapsed time. The tumor volume is calculated as an ellipsoid with a, b, c measured by calipers.

**Results:** Figure 2A plots the measured tumor volume as a function of time. The tumor volume growth exhibited two growth phases: an initial phase with an apparent tumor volume doubling time of about 1.1 days (or 26 hours slightly longer than the in vitro cell doubling time of 20 hours) and a late "slow" phase with an apparent volume doubling time of 2.7 – 2.8 days. The late volume growth is significantly slower than the tumor cell doubling time, reflecting the complex nature of the volume growth which depends on such factors as cell loss, cell supporting matrix, cell death, slow cell division due to shortage of nutrients or oxygen, etc. (file: growth\_ba1112\_031202.xls). Data on the tumor volume growth was accumulated continuously and to followed up for longer time. Figure 2B plots the measured tumor volume as a function of time with the most up-to-date data. The volume doubling time for the late growth phase is determined to be 3 days. (file: XC.08 I-125.xls).

Fitting of the in vivo tumor growth measured in 7/8/91 on the p line (p443, p445, Fig. 3 and 4 respectively) showed a slightly different tumor volume doubling time. The volume doubling time in the late grow phase was 2.5 and 2.9 days for the P445 and P443 lines, respectively. Only the P445 line exhibited two different growth phases. The doubling time for the initial and late phases was 1.6 days and 2.9 days, respectively. It

appears that there was not enough data taken for the tumor growth in the time range of initial growth. For the late growth phase, the volume doubling time obtained from this set of data is consistent with the current data. (file: growth\_p\_line\_070891.xls).

Therefore, the value for the late tumor grow volume-doubling time will be determined as 3.0 days. The initial stage volume doubling time is about 1.1 to 1.6 days, which is slightly longer than the in vitro cell doubling time (20 hours). Since onset of in vivo CLDRI taken place at about 19-21 days, the late phase volume-doubling time will be used for the model calculation. This is valid if the tumor density is assumed to be constant. Cell loss and death and reduced cell proliferation due to short supply of nutrients and oxygen will slow the in vitro cell-doubling rate. The growth of blood vessel and tumor cell supporting matrix complicates the relationship between the cell number and tumor size. (Presumably, the outer layer may grow with cells of in vitro doubling time, but the inner layer which has less sufficient nutrient may have cell number increase less than that of the in vitro doubling time). Since these factors are not taken into account explicitly in the model calculation, the use of the late phase volume doubling time as the cell number doubling time the model calculation is a reasonable approximation, as further supported by the data described next.

c. Tumor cell growth based on in vivo tumor growth and in vitro cell assay

**Methods:** Tumor cells of 4500 to 7500 are inoculated to the head of the rat. Tumors were allowed to grow on the rat until 19 to 21 days. The cells from the tumor at 19 to 21 days were measured by cell assay of the tumor.

**Results:** 1) number of cells measured from the tumors grown on the rat's head at 19-21 days spread from  $1-7 \times 10^6$ ; the measured cell number correlates linearly with the measured volume of the tumor (Fig.5). Therefore, the use of late phase volume doubling time for model calculation is a reasonable one. Because the volume growth as described in 1.b. progress from a fast early to a late slow phase within this period of time, assumption of a simple exponential growth from day of tumor cell inoculation to the elapsed days of 19 – 21 day will not be valid. If this assumption was used, the cell number doubling time estimated from this assay technique ranged from 1.8 to 2.6 days. As expected, it is smaller than late phase doubling time of 3.0 days. (file: cellnumber\_at\_rx.xls).

2. Sublethal damage repair time constant

**Methods:** Split dose experiment was performed with 250 kV x-rays for Ba-1112 cell line. A total dose of 10 Gy was given. The survival fraction was measured as a function of time interval between two 5 Gy irradiation. The cells were kept at 22°C during the waiting interval to prevent proliferation. According to incomplete repair model we have,

$$\frac{\ln[S(t)/S(0)]}{\ln[S(\infty)/S(0)]} = 1 - e^{-\mu t}$$

where  $S(t)$  is the surviving fraction with split time interval  $t$  and  $\mu$  is the sub-lethal damage repair time constant.

**Results:** By fitting the measured data to the above equation (Fig.6), the in vitro repair half-time for the BA1112 cells was determined to be 20 minutes (split\_dose\_ba1112.xls).

### 3. $\alpha$ and $\beta$ for the linear-quadratic cell survival model

**Methods:** The parameters of  $\alpha$  and  $\beta$  for the Ba-1112 cell line for  $^{125}\text{I}$ ,  $^{103}\text{Pd}$ , and 250 kV photons were determined from the survival curves obtained under acute exposure condition using simulated  $^{125}\text{I}$  and  $^{103}\text{Pd}$  x-ray beam on an orthovoltage unit. The animals chosen for the in vitro irradiations of the BA1112 sarcoma cells were euthanasia by anesthetic overdose and the tumor cells were then removed using aseptic techniques. A single-cell suspension of tumor cells was suspended, counted, and assayed for viability using the same colony formation assay used for cells in cultures. The response of tumors to irradiation will be assessed by the ability of the BA 1112 tumor cells to form colonies in cell culture after in vitro irradiations at energies equivalent to  $^{125}\text{I}$  and  $^{103}\text{Pd}$  under aerobic conditions, and leading to exponential growth at different rates (from near quiescence to full exponential growth at a maximal rate).

To obtain the  $\alpha$  and  $\beta$ , the acute survival curves for the simulated  $^{125}\text{I}$ ,  $^{103}\text{Pd}$ , and the 250 kV x-rays were fitted to the LQ cell survival equation. Several factors need to be considered for such a fit. 1) If the actual cell survival fraction is used in the fit, the least square fit will automatically favor the data points with large survival fractions, i.e. survival data at low doses dominates the fitting process. 2) To increase the importance of large dose data points, the logarithms of the survival fractions were used to fit the LQ model. Although it gives an improved fit, it does tend to emphasize the large dose (small survival fraction) data, of which have usually large uncertainties. 3) If the survival curves of  $^{125}\text{I}$ ,  $^{103}\text{Pd}$ , and the 250 kV were fitted individually to LQ equation, the  $\alpha$  and  $\beta$  will assume different values for each beam. It probably represents the best data for each beam, and the use of these parameters in model calculations for each beam characteristics may yield the best agreements with experiments for the given beam. However, it will restrict the model calculation applicable for only the beam characteristics that has the fitted parameters. The model will lose its general predictive power.

Initially, we have taken a two-step fitting procedure. In the first step, the logarithm of the survival data was fitted to the LQ equation individually for each beam. The average of the  $\beta$  from these fits is then used as a fixed parameter for a second fit of log survival curves to determine the  $\alpha$  for each beam. The rationale was that  $\beta$  represents the cell death due to sublethal damages that is intrinsic to each cell line. However, this procedure would lump all dose rate effects to the parameter  $\alpha$ . As a result, it produced quite different  $\alpha/\beta$  ratio for each beam. Since  $\alpha/\beta$  represents the dose at which the cell damage from single hit equals to that from double hits, regardless of dose rates (?),  $\alpha/\beta$  should be kept constant during the fit. The new procedure developed for the parameter fitting is as follows. The log survival fraction from all three beams were used simultaneously in a least square fit in which the  $\alpha$  for each beam and  $\alpha/\beta$  are treated as



the global fitting parameters. The measured survival curves and the calculated curves using the fitted parameters were given in Fig.7A. The  $\alpha$  and  $\beta$  determined by this procedure are given in the following table. The parameters determined from a global fit in which the  $\beta$  was assumed to be the same for all beams is also given for a comparison (Fig. 7B). It is interesting to note that the values of the  $\alpha$  and  $\beta$  determined from these two fitting procedures are not that different. A literature search on the radiobiological parameters on the BA1112 cell line did not yield previously determined parameters for the LQ cell survival model. Further investigation on the process of determine these parameters from the measured survival curves at different conditions is planned.

#### Radiobiological Parameters Determined from Acute Exposure Experiments

Beam	Parameters for Ba-1112				
	$\alpha$ (Gy <sup>-1</sup> )	$\beta$ (Gy <sup>-2</sup> )	$\alpha/\beta$ (Gy)	Tumor Doubling Time (day)	Sub-lethal Damage Repair Half-time (hr)
250 kV old	0.25	0.041	6.1	3.0	0.33
<sup>125</sup> I equivalent	0.26	0.043	6.1	3.0	0.33
<sup>103</sup> Pd equivalent	0.29	0.048	6.1	3.0	0.33
250 kV old	0.23	0.044	5.1	3.0	0.33
<sup>125</sup> I New	0.25	0.044	5.6	3.0	0.33
<sup>103</sup> Pd New	0.32	0.044	7.3	3.0	0.33

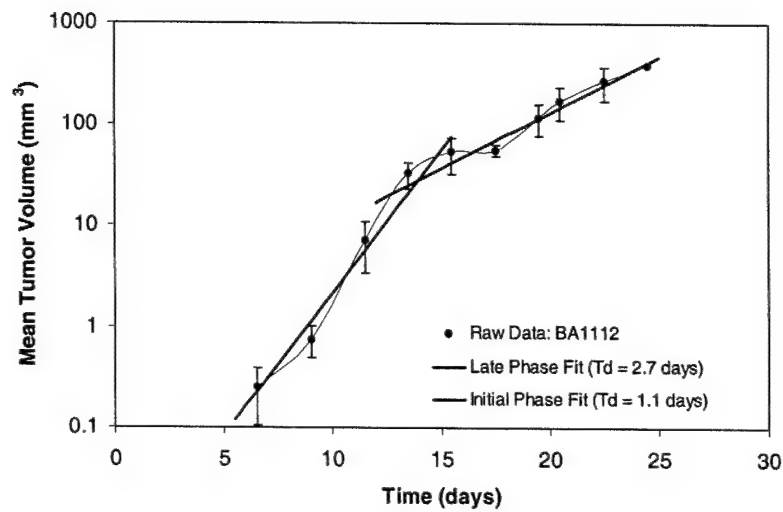


Figure 2

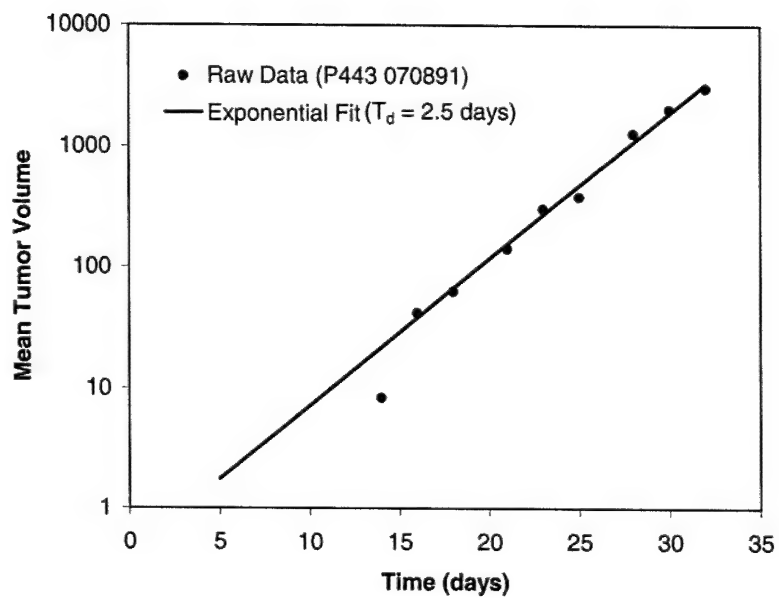


Figure 3

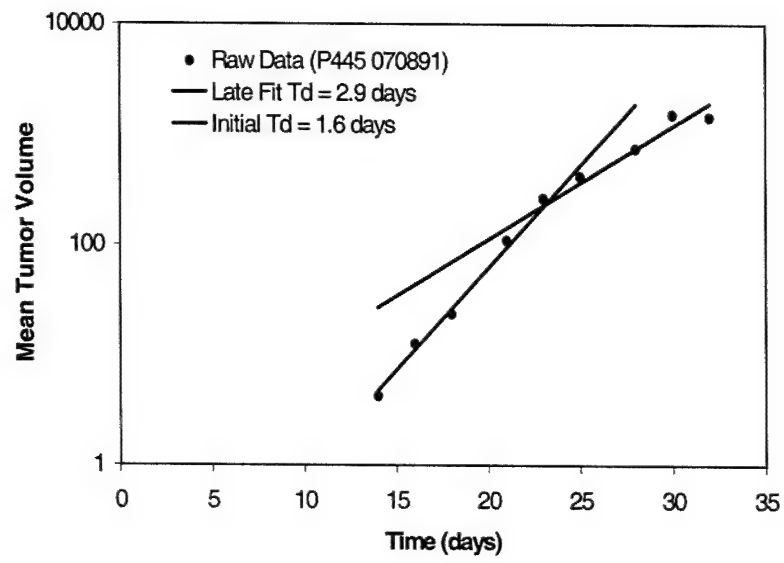


Figure 4

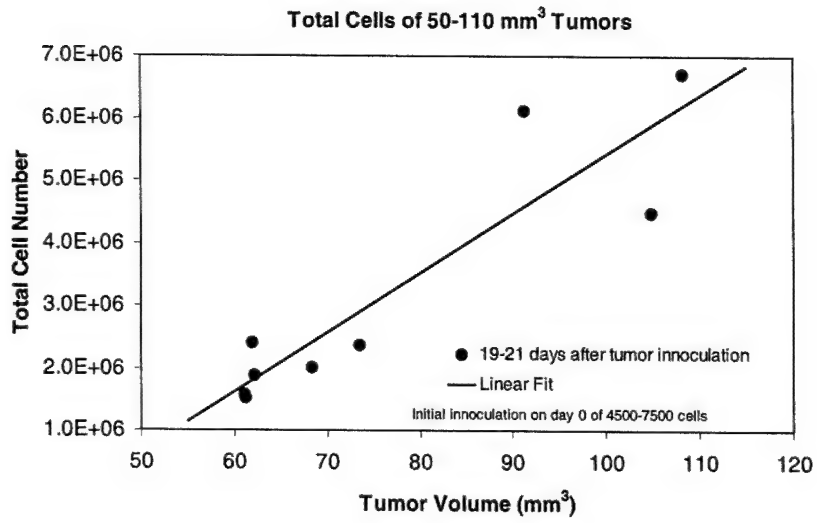


Figure 5

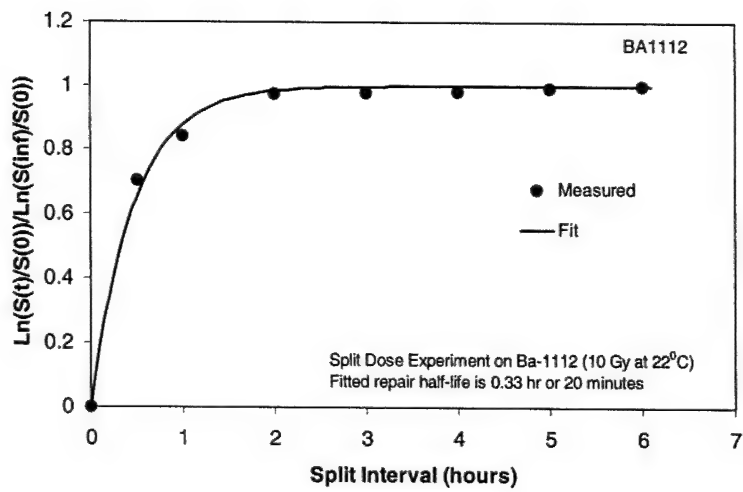


Figure 6

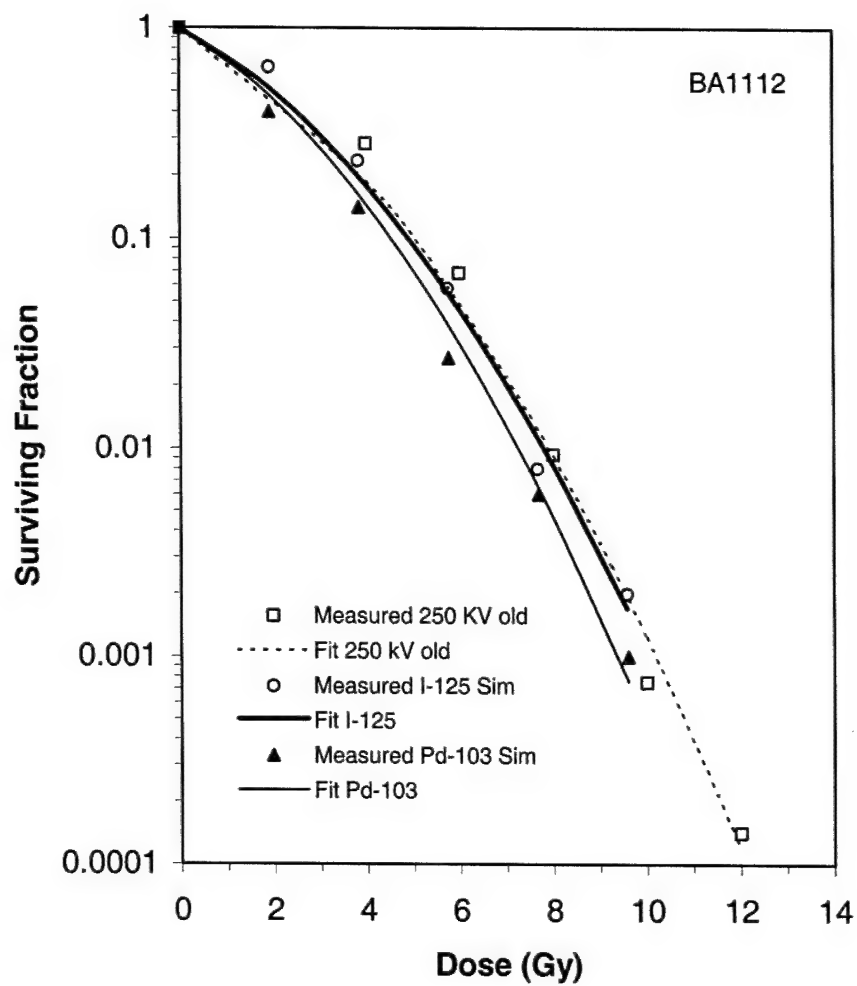


Figure 7

## APPENDIX V

### IN VITRO STAINING PROTOCOL FOR FLOW CYTOMETRY

1. GROW CHO CELLS AS A MONOLAYER @ 37°C IN BME PLUS 15% FBS, VITAMINS, AND P/S. GROW BA-1112 FROM PRIMARY EXPLANT IN D-MEM PLUS 15% FBS, P/S, Na-PYRUVATE, VITAMINS.
2. LET CELLS OBTAIN LOGARITHMIC GROWTH. THEN LABEL CELLS WITH IUDR FOR 24 HRS. IUDR CONCENTRATION FOR LABELLING IS  $10^{-5}$ M &  $10^{-4}$ M IUDR.

PE= NO ANTIBODY TREATMENT, CELLS W/O IUDR

CONTROL= SECONDARY ANTIBODY TREATMENT ONLY, CELLS W/O IUDR

EXPERIMENTAL= PRIMARY/SECONDARY ANTIBODY TREATMENT, IUDR-LABELLED CELLS

3. AFTER 24 HRS INCORPORATION TIME, TRYPSINIZE CELLS, THEN COUNT CELLS AND DISTRIBUTE  $3 \times 10^5$  CELLS/TUBE INTO 5 MICROCENTRIFUGE TUBES. (3-EXP, 1-CON, 1-PE) FIX THE CONTROL AND EXPERIMENTAL TUBES WITH 0.5 ML OF 70% ETHANOL FOR 30 MINUTES ON ICE (4°C). LEAVE PE TUBE IN Pi/NaCL.
4. REMOVE CELLS FROM ETHANOL ( $3 \times 10^6$  CELLS). RESUSPEND INTO 1.0 ML OF 1.5M HCL @ 20°C FOR 20 MINUTES.
5. WASH CELLS TWICE WITH 0.5 ML Pi/NaCL

#### PRIMARY ANTIBODY

6. RESUSPEND IN A Pi/NaCL SOLUTION CONTAINING .5% TWEEN-20, .5% BOVINE SERUM ALBUMIN (MONO I), AND A 1:50 DILUTION OF A MONOCLONAL ANTIBODY (RABBIT ANTI 5 IODOURIDINE) (0.4 ML) FOR 1HR AT ROOM TEMPERATURE (20°C).  
**REMEMBER:** DO NOT ADD THIS ANTIBODY TO THE CONTROL TUBES!
7. WASH CELLS TWICE AGAIN WITH 0.5 ML Pi/NaCL.

#### SECONDARY ANTIBODY

8. RESUSPEND INTO A Pi/NaCL SOLUTION CONTAINING .5% TWEEN-20, 1% NEUTRAL GOAT SERUM (MONO II), AND A 1:100 DILUTION OF FLUORESCIEIN-LABELLED GOAT ANTI-RABBIT IgG (0.4 ML) FOR 30 MINUTES OF ROOM TEMPERATURE (20°C).  
**REMEMBER:** ADD THIS ANTIBODY TO CONTROL AND EXPERIMENTAL TUBES.
9. WASH CELLS AGAIN WITH 0.5 ML Pi/NaCL
10. CELLS MAY BE USED FOR DETERMINATION OF IUDR CONTENT BY PROPIDIUM IODIDE STAINING AND MEASUREMENT BY FLOW CYTOMETRY @ 600nm (RED FLUORESCENCE), OR LUMINESCENCES MEASUREMENTS @ 514nm (GREEN FLUORESCENCE).

### In Vivo BrdU Labeling Protocol For Flow Cytometric Analysis

#### Fixation of Cells in 75% Alcohol (Step 1):

An injection of 50 mg per kg BrdU is given intraperitoneally, and at appropriate times thereafter a rat was sacrificed and the tumor was excised, cut into small pieces, washed with Hanks basic salt solution, and incubated at 37°C for 10 minutes in Hanks solution containing 0.05% trypsin.

The resulting cell suspension was filtered through a 22 nylon mesh filter and centrifuge at 1000 rpm for 5 minutes.

Remove the supernatant without disturbing the pellet.

**FOLLOWING STEPS DONE ON ICE (4°C)**

Add 1.0ml of PBS/EDTA solution and gently stir with the pipetman in order to get the single cell suspension.

Add 4.0ml of PBS/EDTA

Centrifuge at 1000rpm for 5 minutes.

Remove supernatant again without disturbing the pellet

Add 1.0ml of PBS/EDTA solution and gently stir with the pipetman in order to get the single cell suspension.

Now add 1.0ml of 95% ethanol drop by drop, very slowly while vortexing the pellet at a very low speed. (knob setting = 1)

Now add 1.0ml of 95% ethanol drop by drop, very slowly while vortexing the pellet at a very low speed. (knob setting = 2)

Now add 1.0ml of 95% ethanol drop by drop, very slowly while vortexing the pellet at a very low speed. (knob setting = 3)

**SUMMARY NOTE:** 3.0ml of 95% ethanol should be added in three steps, 1.0ml at each step drop by drop while vortexing the pellet. The only difference is the increase in the vortex speed from 1 to 3.

The tube has now 4.0ml of volume (1.0ml of PBS/EDTA and 3.0ml of 95% ethanol. (final concentration of alcohol is 75%)

**REMEMBER:** All the steps above must be done on ice, including putting the alcohol on ice before starting.

**NOTE:** You can keep the cells at 4°C for one month until proceed to the next step.

**Neutralization of Cells (Step 2):**

Centrifuge the cells @ 1500 rpm for 10 minutes.

Remove the supernatant without disturbing the pellet.

Add 1.0ml PBS/EDTA slowly drop by drop while vortexing the pellet gently. (Do not use the pipetman here because you will lose cells.)

Add 4.0 ml of PBS/EDTA to bring final volume to 5.0 ml.

Centrifuge at 1500 rpm for 10 minutes.

Remove supernatant with a Pasteur pipette.

Vortex the pellet.

Add 1.0ml of 2N HCL/ 0.5%TritonX-100 drop by drop while vortexing at low speeds.

Let sample sit at room temperature (20-25°C) for 30 minutes.

Centrifuge at 1500 rpm for 10 minutes.

Remove supernatant.

Add 1.0ml of 0.1M sodium tetraborate ( $\text{Na}_2\text{B}_4\text{O}_7 \cdot 10\text{H}_2\text{O}$ ) ph 8.5 drop by drop while vortexing pellet at setting 2.

Centrifuge @ 1500 rpm for 10 minutes.

Remove supernatant.

Add 1.0ml of PBS/0.5%Tween-20/1%BSA solution drop by drop while vortexing the cell pellet.

**NOTE:** You can keep the cells at 4°C until the next day.

‡ **Staining The Cells with Anti-BrdU Antibody (Step 3):**

Centrifuge @ 1500 rpm for 10 minutes

Remove supernatant.

Add 200 ul of PBS/0.5%Tween-20/1%BSA solution. The tumor cells are rinsed three times with this solution before incubation with primary antibody.

Centrifuge @ 1500 rpm for 10 minutes after last rinse

Add 0.5ml of the primary antibody to BrdU (rat monoclonal Anti-BrdU antibody 1:100 dilution with PBS/.05%Tween-20/1% BSA solution).

Incubate for 60-90 minutes at room temperature, 25°C, with a gentle tapping of the tubes every 15 minutes to get uniform staining of all cells.)

Wash cells twice again with 0.5 ml of PBS/0.5%Tween-20/1%BSA solution.

Centrifuge @ 1500 rpm for 10 minutes.

Remove supernatant.

For the secondary antibody incubation, resuspend the 0.5ml of the fluorochrome-conjugated antibody, (goat anti-rat antibody, 1:200 dilution in PBS/.05%Tween-20/1% BSA solution) at room temperature, 25°C for 45 minutes.

Wash cells again with 0.5 ml of PBS/.05%Tween-20/1% BSA solution.

**Propidium Iodide Staining- Cellular DNA Content (Step 4):**

Centrifuge, decant or aspirate fixative. Insure all ethanol has been removed leaving tube upside down o a paper towel

Resuspend cells in RNase at  $2 \times 10^6$  cells or minimum of 0.4 ml. Incubate at 37°C for 30 miutes.

Add Propidium Iodide for a final concentration of 0.05 mg/ml. Keep at 4°C for a least 45 minutes prior to flow cytometric analysis.

Filter samples thorough a 35 micron nylon mesh immediately prior to analysis.



Development of a Rat Solid Tumor Model for Continuous Low Dose Rate Irradiation  
Studies using  $^{125}\text{I}$  and  $^{103}\text{Pd}$  Sources

Ravinder Nath, Paul Bongiorno, Zhe Chen, Jillian Gragnano, and Sara Rockwell

Department of Therapeutic Radiology, Yale University School of Medicine, 333 Cedar  
Street, New Haven, Connecticut 06510

(Submitted to International Journal of Brachytherapy on )

Supported in part by DOD grant no. DAMD 17-00-1-0052, awarded by the Department  
of Army

## Abstract

An experimental technique for radiobiology studies of brachytherapy continuous low dose rate irradiation (CLDRI) using a rat solid tumor model has been developed. BA1112 tumors were grown between the ears of the 14-week old male WAG/rij rats by interdermal inoculation. Irradiation of the tumor, in vivo, by the  $^{125}\text{I}$  and  $^{103}\text{Pd}$  brachytherapy sources was accomplished by using source afterloading system, which consists of a lightweight helmet sutured to the rat and a nine-source afterloading applicator. The applicator, made of clear polystyrene with loading ports for nine sources, has a 12 mm  $\times$  12 mm opening in the center to accommodate the tumor and its growth during the irradiation (the diameter of a typical BA1112 tumor is about 6 mm when radiation is applied). The spatial location of the nine sources were optimized to produce an as uniform as possible three-dimensional dose distribution to the central portion of the applicator for both  $^{125}\text{I}$  and  $^{103}\text{Pd}$  sources. Absolute dose delivered by the applicator was verified by point dose measurements using calibrated TLD in a polystyrene phantom that mimics the scattering environment of the tumor on the rat. This experimental technique was applied to study the in vivo response of the BA1112 tumors to  $^{125}\text{I}$  and  $^{103}\text{Pd}$  treatment, by measuring the tumor size twice weekly during the treatment until each tumor has reached a maximum volume of 1 cm<sup>3</sup> or until the tumor has regressed and the animal has been free of tumor for 100 days. The technique was also applied to for tumor cure studies under CLDRI by measuring the cell survival in vitro following in vivo irradiation of the tumor. In this application, BA1112 tumors were irradiated at a low dose rate in vivo to graded doses from 2 to 20 Gy, the tumours were then removed and their colony formation ability was measured using an in vitro assay techniques. (explicit results) Description of the technique and its application for brachytherapy radiobiological studies are presented.

length) x 2.15 cm (side-side width) x 2.2 cm (height). Prior to irradiation, the helmet was sutured to the rat's head by four stitches through the cartilage of the ears and two more stitches just behind the head at the neck (Fig.1). A seventh suture placed under the tumor will be tied to the central bar that across the top of the helmet, thus ensuring the tumor is pulled up into the center of the treatment volume. Radioactive sources of  $^{125}\text{I}$  or  $^{103}\text{Pd}$  were loaded into the afterloading applicator in the hot lab and the applicator was then transported to the animal facility to be afterloaded into the helmet.

Because the CLDRI experiment lasts over a long period of time, special radiation shielded animal housing was built with transparent Pb-plastic door, which provides adequate light and air for the rats during the long irradiation. The experimental protocol was reviewed and approved by the Yale University Animal Care and Use Committee prior to the start of the experiments. The attachment of the helmets and gesturing during the long irradiations has shown no ill effects on the animals. The rats have gained weight as expected and have gone on their daily activities.

#### BA 1112 tumor model characteristics

Tumors used for in vivo tumor cure studies have been implanted by the subcutaneous inoculation of about 5000 tumor cells into the subcutaneous tissues between the ears of 14-week-old male WAG/rij rats. The cells were obtained from a single cell suspension of BA1112 cells harvested from the BA1112 tumor growing on the head of a previously inoculated rat at an elapsed time of about 21 days. The rats are bred and maintained in our breeding colony under SPF conditions. (Brief description (or reference) of the BA1112 tumor cell line and its characteristics and suitability for brachytherapy radiobiology studies).

Figure 3 plots the measured tumor volume as a function of time. The tumor volume growth exhibited two growth phases: an initial fast growing phase and a late slow phase. From an elapsed time of 15 days on, the tumor volume grow exponentially with an apparent volume doubling time of about 3 days. The late volume growth rate is significantly slower than the in vitro tumor cell doubling time (about 20 hours), reflecting the complex nature of the volume growth that is affected by such factors as cell loss, cell death, prolonged cell cycle due to local environment as well as the supply of nutrients from the tumor cell supporting matrix.

#### Tumor cure studies under $^{125}\text{I}$ and $^{103}\text{Pd}$ CLDRI

Two techniques have been developed to study the tumor response to brachytherapy CLDRI treatment using  $^{125}\text{I}$  and  $^{103}\text{Pd}$  sources. In the first approach, irradiation of the tumor was applied at about day 21 since the inoculation of the tumor cells to the rat. Typical tumor volume at onset of radiation is about 100-200 mm<sup>3</sup>. The response of the tumors to CLDRI was analyzed by measuring the tumors twice weekly during the irradiation until each tumor has reached a maximum volume of 1 cm<sup>3</sup> or until the tumor has regressed and the animal has been free of tumor for 100 days. The pattern of tumor growth was analyzed and TCD<sub>50</sub> were calculated for comparing the effects of different treatments.

In the second approach, an in vitro tumor cell survival assay from tumor irradiated in vivo was used. Irradiation of the tumors growing on the rats, to different radiation dose, commenced at approximately 3 weeks after inoculation. The rats were killed at the end of the irradiation and the tumor cells were suspended, counted, and assayed for viability using the same colony formation assay used for cells from cultures. Analyses of cell yield were performed to allow for the loss of cells during the protracted irradiations. This endpoint was used to measure the cell survival curves after relatively short, graded treatment times (hours to days).

Experiments were conducted using  $^{125}\text{I}$  sources with mean initial dose rate of 8 cGy/hr and 16 cGy/hr, respectively. For  $^{103}\text{Pd}$  sources, a mean initial dose rate of 16 cGy/hr was used.

## Results and Discussion

The intrinsic initial iso-dose-rate distributions (in cGy/hr) in the planes parallel to the base of the applicator for sources of unit air-kerma strength are shown in Fig. 4 for  $^{125}\text{I}$  seeds (Draximage model LS-1) and in Fig. 5 for  $^{103}\text{Pd}$  (Theragenic Model 200) seeds. Eight representative planes parallel to the base of the applicator, located at -1mm (A), 0mm (B), 1mm (C), 2mm (D), 3mm (E), 4mm (F), 5mm (G), and 6mm (H) above the base, are shown in each graph. Figure 6 plots the cumulative dose-volume histogram for a cylindrical volume at the center of the applicator (the cylinder has diameter of 10 mm and a height of 10 mm). It is seen that the iso-dose-rate distribution inside the open portion of the application has a uniformity between 95% and 150% for both  $^{125}\text{I}$  and  $^{103}\text{Pd}$  seeds. Table I compares the dose measured in polystyrene to the dose calculated to water at the same measurement point for six applicators. The measured dose in polystyrene is on the order of 5% higher than the calculated dose.

Figure 7 and 8 show tumor growth under CLDRI for  $^{125}\text{I}$  with initial dose rate of 8 cGy/hr and 16 cGy/hr, respectively. At the initial dose rate of 8 cGy/hr, the tumors were not cured. However, the tumor growth was slowed from a volume-doubling time of 3 days to an apparent volume-doubling time of 21 days under CLDRI. When the initial dose rate is increased to 16 cGy/hr, tumor cure was observed for the initial four animals. The experiments on four more animals are being conducted which will complete by the end of June, 2003. The preliminary data indicates that there is a 75% tumor cure for the BA1112 tumor when irradiated by  $^{125}\text{I}$  with initial dose rate of 16 cGy.

Figure 9 plots the similar in vivo tumor cure study for the  $^{103}\text{Pd}$  sources with initial dose rate of 16 cGy. The tumor cure rate is 50% based on the initial experiments.

Figure 10 plots the tumor growth as a function of treatment time when the tumor was irradiated by a mixture of  $^{125}\text{I}$  and  $^{103}\text{Pd}$  sources. The total initial dose rate was 16 cGy/hr with  $^{125}\text{I}$  and  $^{103}\text{Pd}$  each contributing 8 cGy/hr. Under this condition of CLDRI, the tumor cure rate was 75% from the preliminary data.

Figure 11 shows a comparison of the surviving fraction as a function of dose calculated for the BA1112 cells to that measured in an in vivo/in vitro experiment using CLDRI  $^{125}\text{I}$  irradiation with initial dose rate of 8 cGy/hr. The solid line represent the calculated survival curve using the average initial dose rates used in the experiments. The open circle represent calculation using the actual initial dose rate for each experiment. The parameters of  $\alpha$ ,  $\beta$ , repair half-time, and tumor doubling time were determined directly from the measurements performed on the BA1112 cells (details are provided separately). Theoretical prediction based on the in vivo/in vitro cell survival curves is being investigated.

## Conclusion

The experimental technique developed in this work was successfully applied to study the tumor cure of BA1112 tumor under CLDRI using the brachytherapy sources of  $^{125}\text{I}$  and  $^{103}\text{Pd}$ . Many interesting radiobiological issues related to the brachytherapy treatment and its efficacy can be studied using the experimental technique developed here.

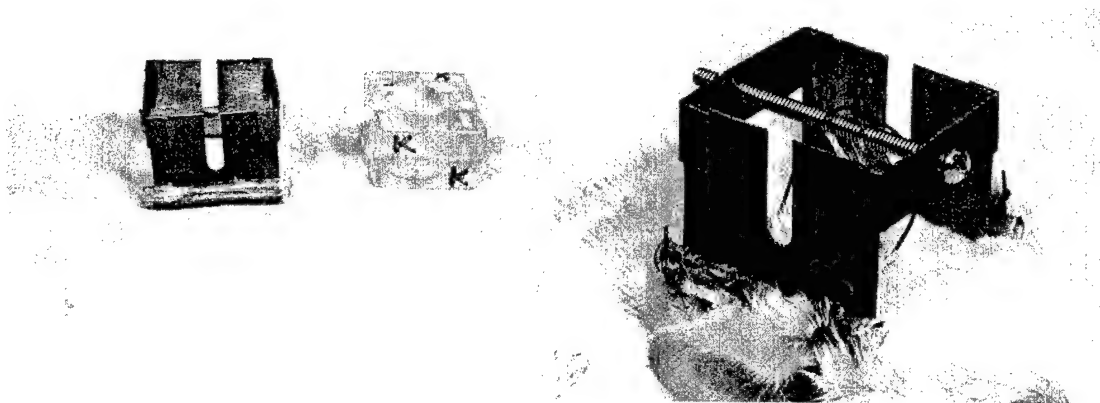
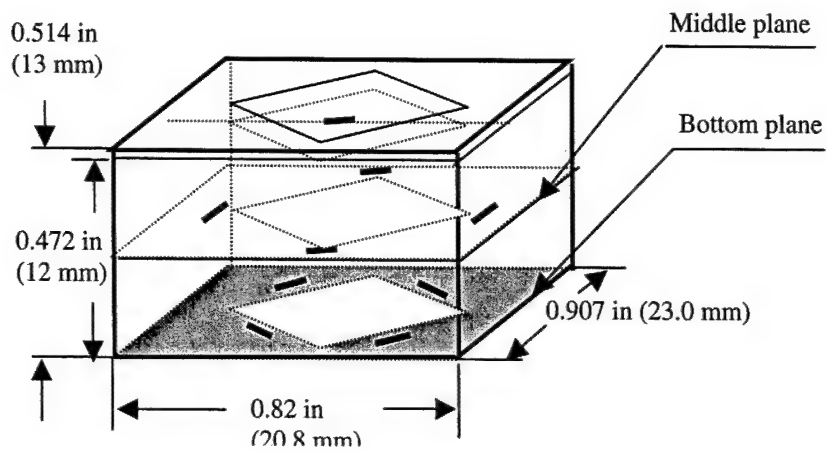
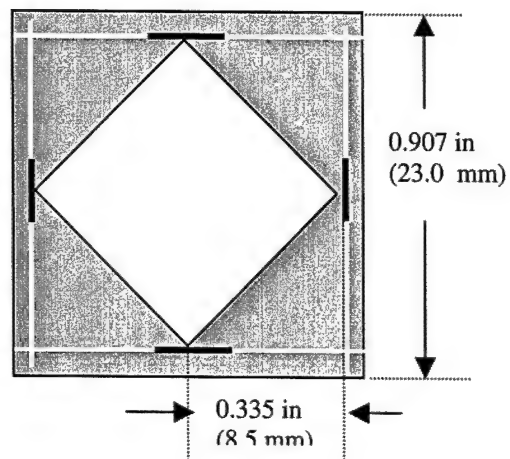


Figure 1, source afterloading system



Middle Plane:  
(0.236 in (6mm)  
from bottom)



Bottom plane:  
(0.039 in (1 mm)  
from bottom)

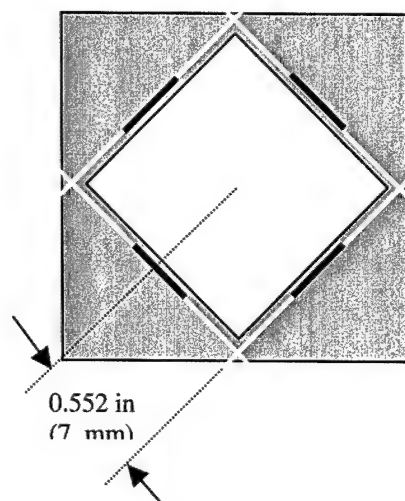


Figure 2:  $^{125}\text{I}$  and  $^{103}\text{Pd}$  afterloading applicator

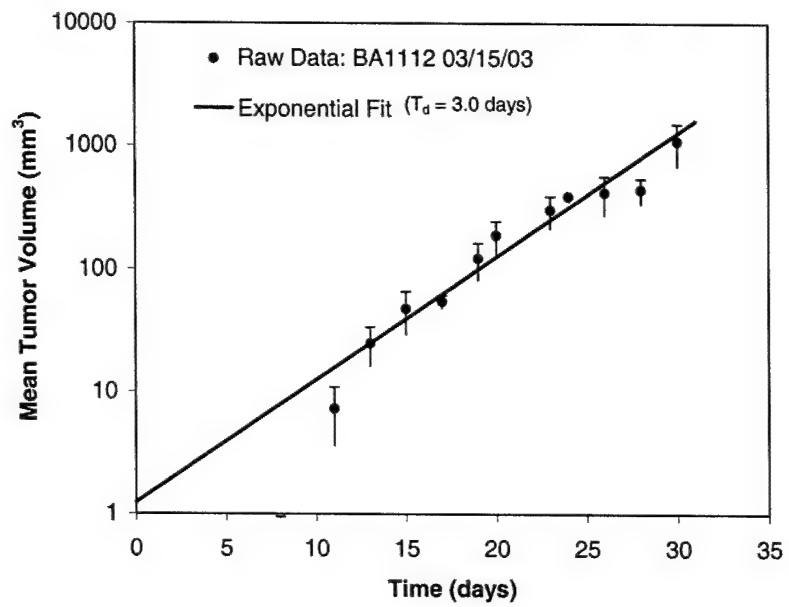


Figure 3



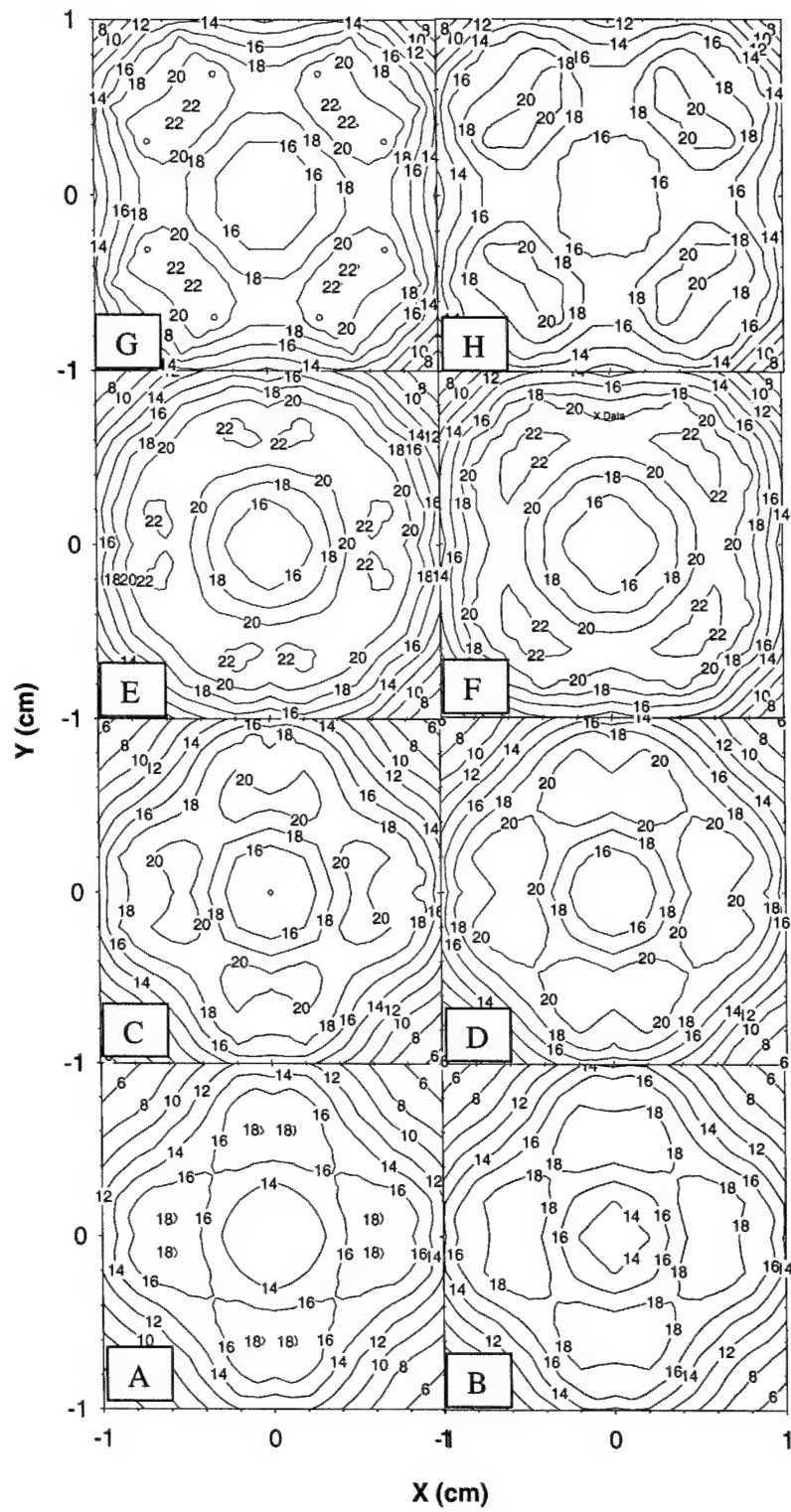


Figure 4: I-125

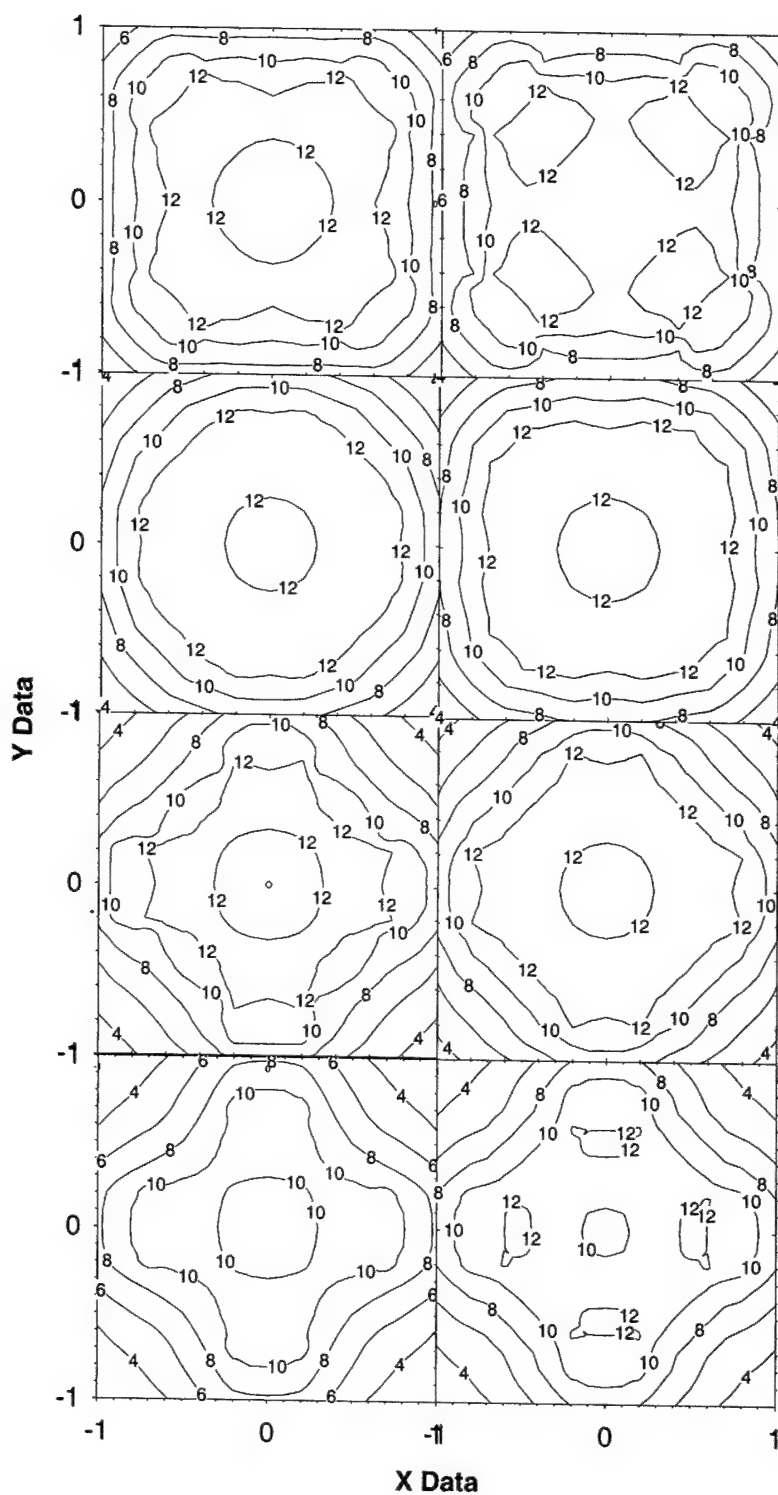


Figure 5: Pd-103

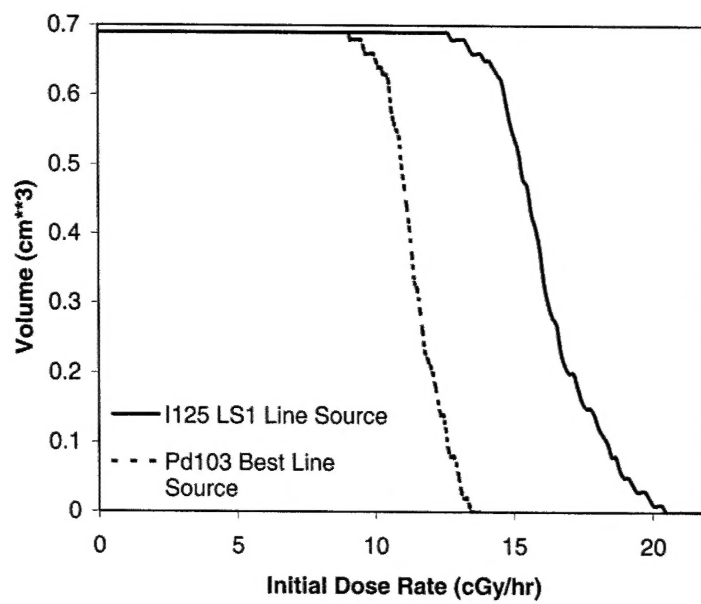


Figure 6

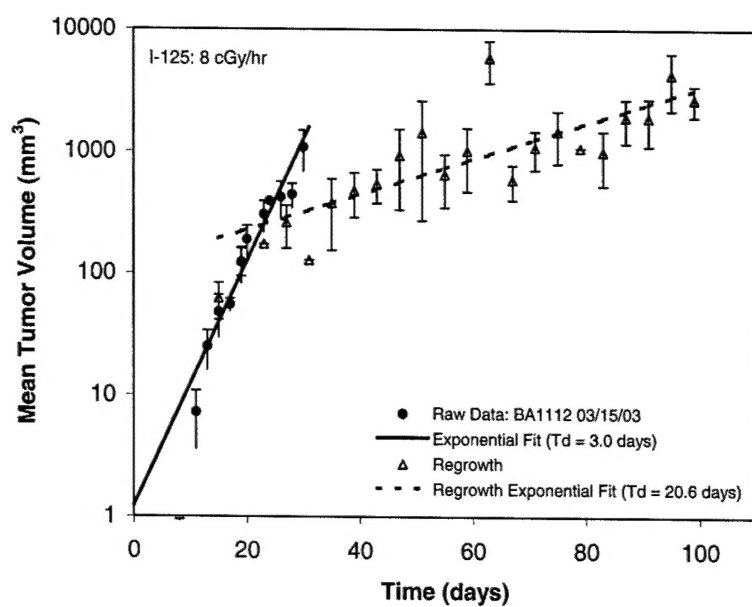


Figure 7

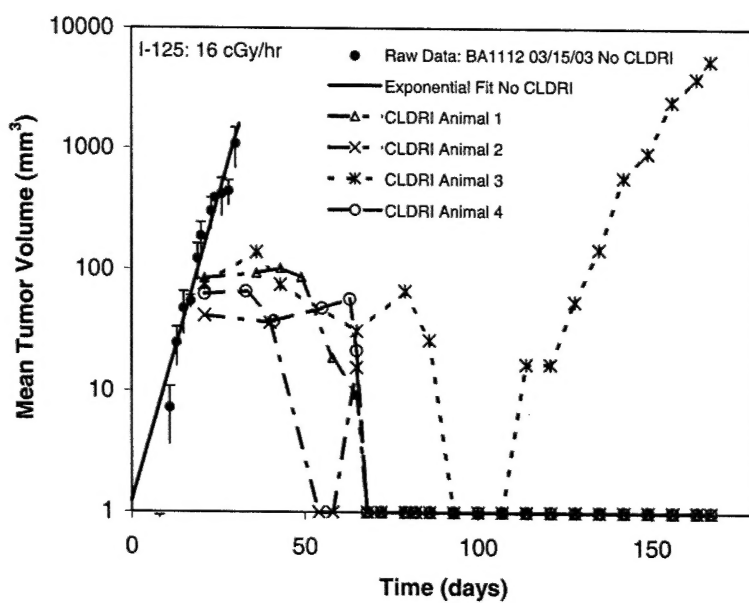


Figure 8

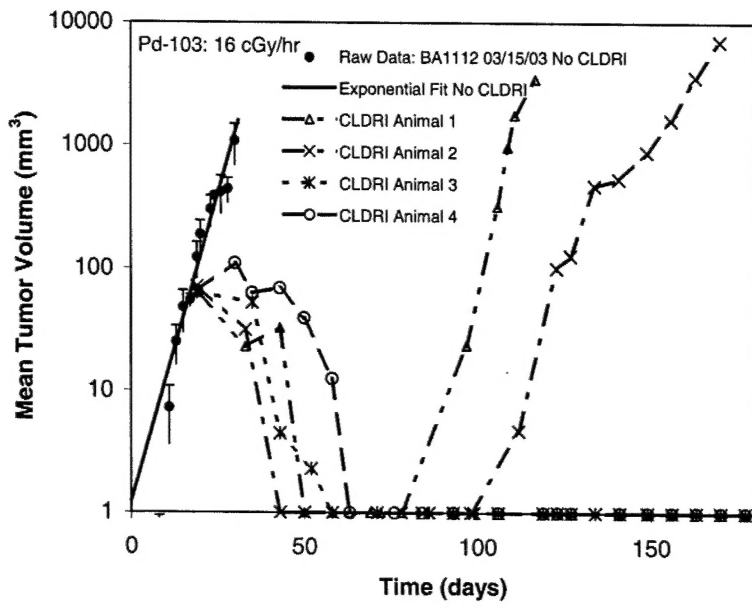


Figure 9

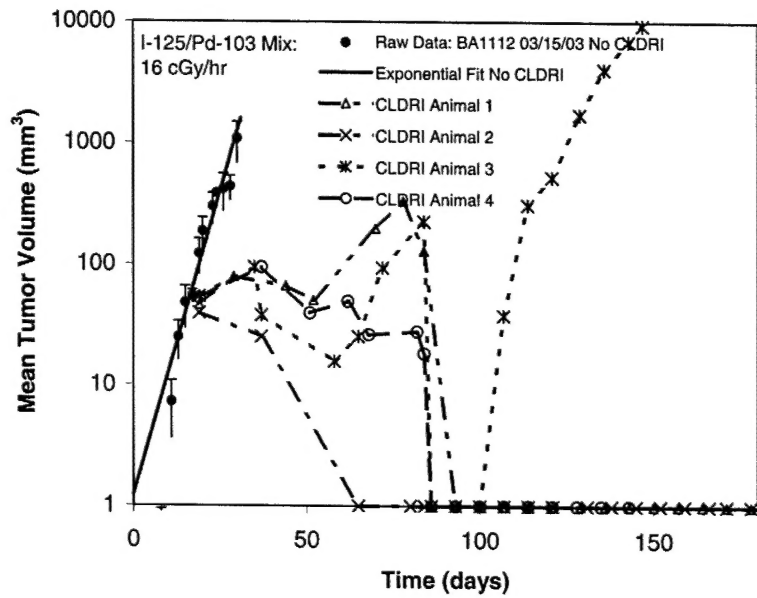


Figure 10

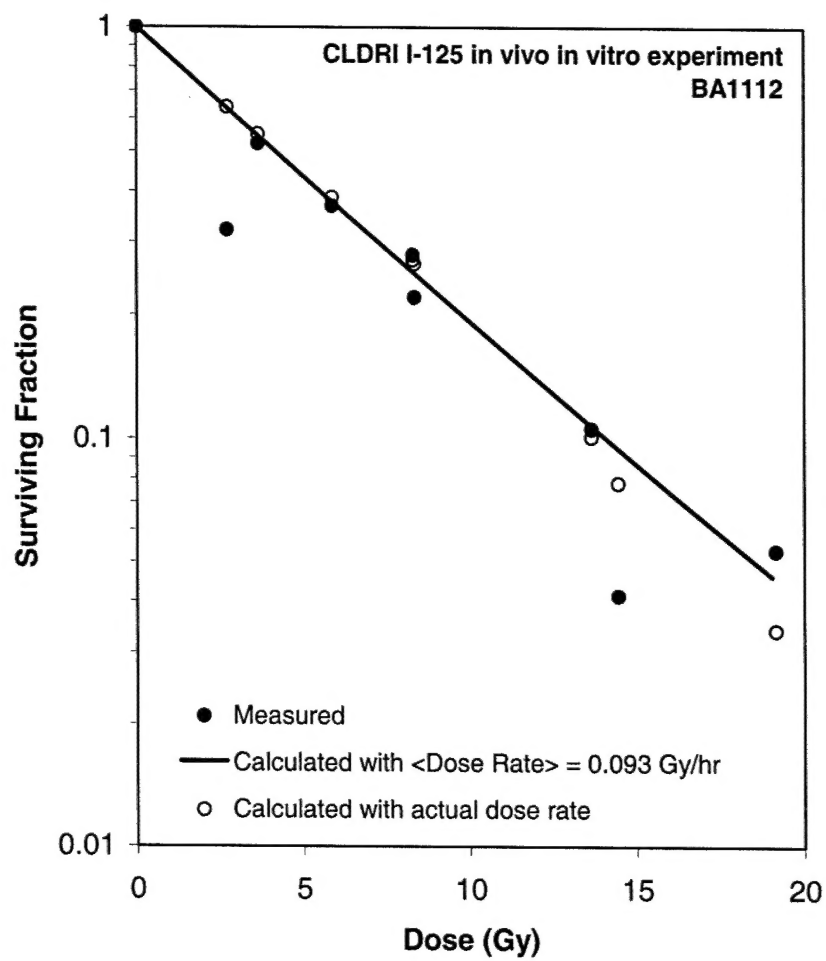


Figure 11